TN272 Cruise Report

Nov. 5 - Dec. 17, 2011
Honolulu, HI – Guam
R/V Thomas G. Thompson

Collaborative Research: A deep-AUV magnetic and seismic study of the Hawaiian Jurassic crust - the global significance of Jurassic magnetic anomalies
(NSF-OCE 1029965)
Chief Scientist: Masako Tominaga

Table of Contents

Tables

Appendices

Cover Image:
Sentry surfacing in the search light during the vehicle recovery effort after the Dive 134.
Photo Credit: W. C. Koeppen

TN272 Roster

Science Party

PIs
Masako Tominaga, Woods Hole Oceanographic Institution (Chief Scientist)
Maurice A. Tivey, Woods Hole Oceanographic Institution (Co-chief Scientist)
Adrienne J. Oakley, Kutztown University of Pennsylvania (Geophysics team leader/Seismic)

Geophysics
Thomas P. Bond, Kutztown University of Pennsylvania (Geophysics Watchstander)
Rachel A. Gipe, Purdue University (Geophysics Watchstander)
Christie Hegemiller, Woods Hole Ocenaographic Institution (Geophysics Watchstander)
Jennifer A. Herting, Kutztown University of Pennsylvania (Geophysics Watchstander)
J. Nicholas Matthews, Kutztown University of Pennsylvania (Geophysics Watchstander)
Danielle K. Moyer, Kutztown University of Pennsylvania (Geophysics Watchstander)
Matthew Sabetta, Kutztown University of Pennsylvania (Geophysics Watchstander)
Ashley M. Stinson, University of Maine (Geophysics Watchstander)

Media/Outreach Coordinator
William C. Koeppen, Earth and Ecological Science Institute

Seismic
Stephen A. Swift, Woods Hole Oceanographic Institution (Seismic Refraction Specialist)
Jinchang ("Sam") Zhang, Teas A&M University (Seismic Reflection Specialist)

Sentry AUV
Andrew S. Billings, NDSF, Woods Hole Oceanographic Institution
Justin K. Fujii, NDSF, Woods Hole Oceanographic Institution
Carl L. Kaiser, NDSF, Woods Hole Oceanographic Institution
James C. Kinsey, NDSF, Woods Hole Oceanographic Institution
Stefano Suman, NDSF, Woods Hole Oceanographic Institution
Korey Verhein, NDSF, Woods Hole Oceanographic Institution

SIO Seismic
E. Lee Ellet, Scripps Institute of Oceanography (Shipboard Geophysics/Seismic)
Gary L. Friedrichsen, Scripps Institute of Oceanography (Protected Species Observer)
Bridget M. Hass, Scripps Institute of Oceanography (Shipboard Geophysics/Seismic)
Julie O'Hern, Scripps Institute of Oceanography (Protected Species Observer)
James C. Turnbull, Scripps Institute of Oceanography (Shipboard Geophysics/Seismic)
Bridget H. Watts, Scripps Institute of Oceanography (Protected Species Observer)

Marine Research Technicians
Brandi M. Murphy, University of Washington (lead tech)
Steven R. Jalickee, University of Washington (2nd tech)

Ship's Crew

Patrick J. Donovan, Master

Eric T. Haroldson, Chief Mate
David J. Vander Hoek, 2nd Mate
Lucas M. Shuler, 3rd Mate
Robert D. Worrad, AB
Ezaquel E. Machado, AB
Pamela J. Blusk, AB
Brian W. Clampitt, AB
India M. Grammatica, OS
Carlos S. Oliveira, AB (cadet)

Terrence S. Anderson, Chief Engineer
James T. Swanton, 1st Assistant Engineer
Michael W. Koch, 2nd Assistant Engineer
David A. Bartell, 3rd Assistant Engineer

Victoria R. Simms, Oiler
Leo A. L. Gabriel, Oiler
Marlo S. Yordan, Oiler
William E. Kinnear, Wiper

Sarah L. Wicker, Chief Steward
Antony T. Balbon, 2nd Chef
Terence Singerline, Mess Attendant.

TN272 Cruise Prospectus
Scientific Rationale

The geomagnetic field has varied in its direction and intensity throughout Earth's history on a variety of timescales. This behavior allows us to constrain not only the physical mechanisms required to generate a planetary magnetic field, but also allows us to use this past field history as a timescale to date geologic events. Marine magnetic anomalies, as recorded in oceanic crust, have played a central role in documenting Earth's magnetic field history, at least over the past 180 My. The oldest part of this record, the Jurassic Quiet Zone (JQZ), prior to 157 Ma (pre-M29 chrons), stands out as a unique period in terms of magnetic field behavior.

The JQZ appears to be a period when field intensity was decreasing rapidly (Cande et al., 1978; McElhinny and Larson, 2003), while reversal rate was apparently increasing. Based on 2002-2003 deep-tow magnetic survey results from the Japanese lineations in the western Pacific Jurassic crust, we believe the lack of measureable anomalies in this oldest ocean crust record is a consequence of both weak field intensity and a high reversal rate. This deep-tow survey also found a period (162.5 to 167 Ma, Chrons M38 to M41) of apparently incoherent anomalies with short-wavelengths and anomalously low amplitudes called the LAZ or Low Amplitude Zone (Tivey et al., 2006; Tominaga et al., 2008). It is unknown if the LAZ is the result of local tectonic or crustal complications or if it truly represents geomagnetic field behavior, in which case it represents a unique period of geomagnetic field behavior when Earth's magnetic field was in a prolonged unstable, perhaps non-dipolar state. While terrestrial magnetostratigraphy provides some support for the rapid polarity reversal nature of the late Jurassic (M25-M38), there are no comparable records of this LAZ behavior.

To test whether the LAZ period is truly a globally significant event we must obtain magnetic records from Jurassic crust formed at a different spreading center (i.e. a conjugate side of the Pacific-Phoenix-Izanagi triple junction). The western Pacific Jurassic crust offers the best opportunity to obtain a coherent sequence of magnetic signals with three sets of magnetic lineations (Japanese, Hawaiian and Phoenix) converging on an area centered at 12°N and 160°E (Fig. 1). The Japanese lineations were targeted by both aeromagnetic (Handschumacher et al., 1988) and deeptow magnetic surveys (Sager et al., 1998; Tivey et al., 2006; Tominaga et al., 2008) and provide the basis for comparison. The Hawaiian lineations offer the next best choice of obtaining a Jurassic anomaly record. Larson and Hilde (1975) used the Hawaiian lineations as the basis for their M-series magnetic anomaly correlations, which was subsequently extended to M25 and M29 by Cande et al. (1978); Nakanishi et al., (1989, 1992); and Channell et al. (1995). Like the Japanese lineations, the sea surface magnetic signal becomes difficult to correlate in the pre M25/M29 chrons of the Hawaiian lineations and the reasons are similar. The water depth is great (ca. 6000 m), the region is equatorial and so subject to greater diurnal noise from the equatorial ring current, and the field strength is weakest at the equator. These effects compounded by what we believe to be a rapidly reversing magnetic field with weak overall amplitude leads to difficult-to-measure magnetic field signals from sea surface vessels.

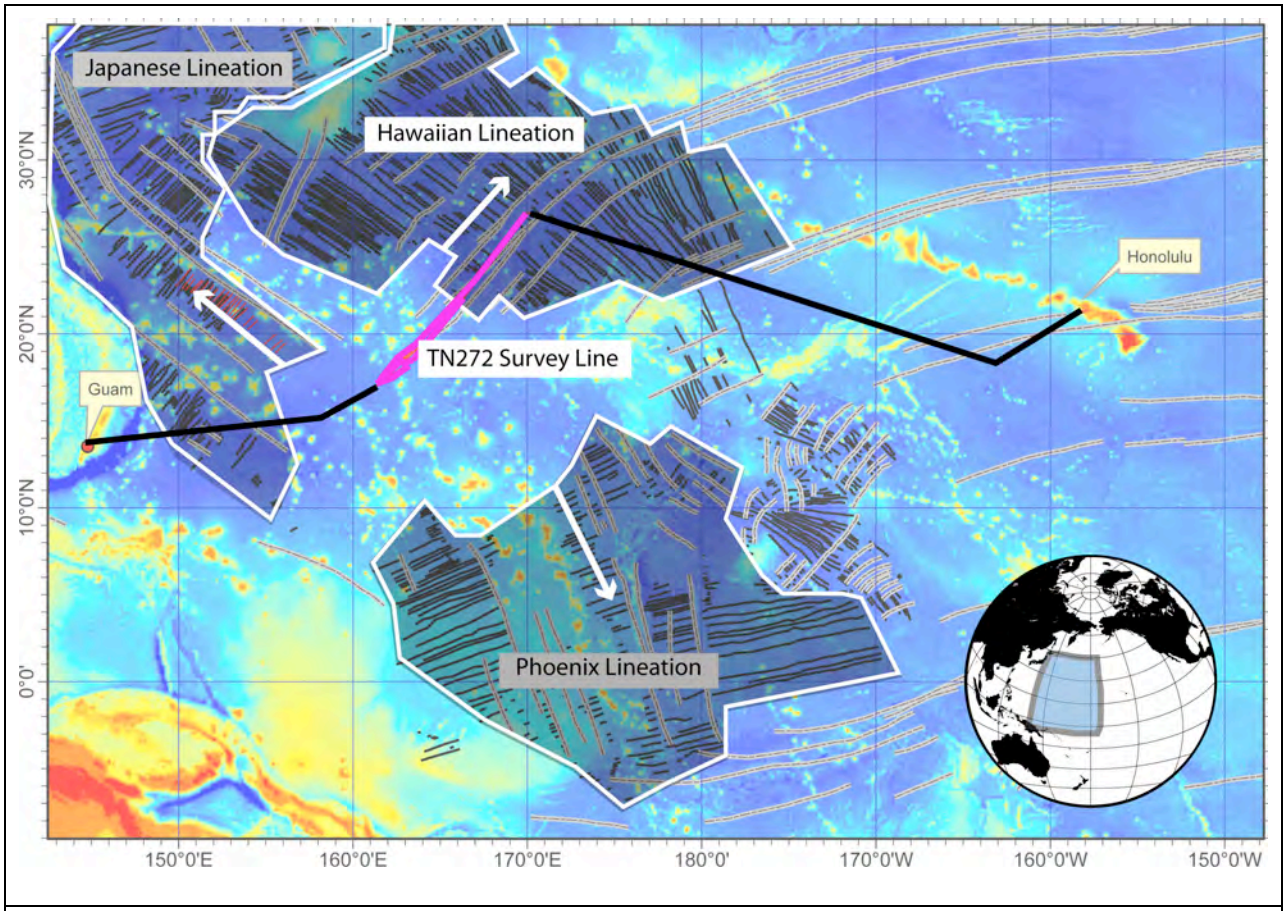

Figure 1. Satellite bathymetry map of western Pacific showing the three sets of magnetic lineations that define the boundaries of the Jurassic crust. The TN272 cruise track is shown by bold black line from Honolulu to Guam. The purple bold line indicates the surveyed Hawaiian lineation sequence.

Scientific Background

History of Earth's Geomagnetic Field

The geomagnetic field displays one of the largest dynamic ranges of Earth's physical properties, varying in intensity and direction on timescales from seconds to millions of years (Courtillot and Le Mouël, 1988). Short (<1 sec) field variations are generally attributed to solar, orbital and Earth's magnetospheric variations (Jacobs, 1959; Onwumechili, 1967; Campbell et al., 1985) while longer field variations (> a few years) are attributed to Earth's internal geodynamo (Elsasser, 1946; Bullard, 1949). Over the past two decades, numerical and laboratory models have been developed that successfully reproduce Earth's geomagnetic field behavior on a basic level complete with spontaneous polarity reversals (Love and Gubbins, 1996; Glatzmaier, 1999; Constable, 2003; Takahashi et al., 2005; Berhanu et al., 2007; Ravelet et al., 2008; Pétrélis et al, 2009; Driscoll and Olsen 2009; Olsen and Driscoll, 2009). The better we can define the past history of geomagnetic field behavior, the better we can inform these geodynamo models to reproduce an accurate

model response and thereby provide insight into the mechanisms that drive the geodynamo and its proclivity for polarity reversal. The geologic record has provided evidence that for most of Earth's history the geomagnetic field has been reversing polarity (Layer et al., 1996; Algeo, 1996; Irving and Parry, 1963; Johnson et al., 1995; Khramov and Rodionov, 1980; Trench, 1991) and varying in geomagnetic field intensity (e.g., Biggin and Thomas, 2003; Tauxe et al., 2006). By combining the geomagnetic intensity and reversal records, many studies have investigated the possible correlation between reversal rates and the dynamics of the geodynamo process (Gallet and Hulot, 1997; McFadden and Merrill, 2000; Lowrie and Kent, 2004; Pétrélis et al., 2009), the correlation between intensity and reversals (Merrill and McFadden, 1999), and even a possible link between the Earth's magnetic field and climate change (Courtillot et al., 1982; Le Mouël et al., 2005; Gallet et al., 2005; Courtillot et al., 2007; Bard and Delaygue, 2008; Courtillot et al., 2008). Thus, by improving our measurements of Earth's past field behavior we can advance our understanding of Earth's processes.

While terrestrial records have given us important insight into past geomagnetic field behavior, our best and most comprehensive record by far has been from the magnetic record of seafloor spreading magnetic anomalies, which extend back in time to ~180 Ma (Fig. 2). The existing GPTS is well-defined from the present back to Chron M29 time, but it is very poorly constrained prior to this period. The marine magnetic record not only allows us to build a continuous and detailed timescale reference frame, but to also accurately quantify reversal rates and to define the relationship between reversals and field intensity fluctuations as a measure of overall geomagnetic field behavior. While the 180 Ma marine record of geomagnetic field behavior shows almost continuous polarity reversal there are two prolonged periods that show quite different behavior. One period is the well-documented Cretaceous Normal Superchron (CNS) from 84-124 Ma, when the field had a constant polarity that is confirmed by its global occurrence in the marine record and also by the magnetostratigraphic record. The second period of unusual geomagnetic field behavior is the more poorly known Jurassic Quiet Zone (JQZ) (>155 Ma), when the reversal rate may have been higher than at any other time (Tivey et al., 2006). The JQZ period provides a much different picture of field behavior compared with the CNS period. Reversal rates decrease into the CNS and then increase after the CNS (Lowrie and Kent, 2004; Valet et al., 2005; Coe and Glatzmaier, 2006), while field intensity appears strong (Biggin and Thomas, 2003; Tauxe et al., 2006). The JQZ on the other hand has high reversal rates while field intensities are low (Tominaga et al., 2008). This fundamental dichotomy makes it important that we capture and quantify this period in Earth's magnetic field history in order to fully understand the full spectrum of geomagnetic field behavior.

The Late-Mid Jurassic (155-180 Ma) Magnetic Anomalies

Mesozoic (M-series) marine magnetic anomalies were first mapped and correlated in the northeast Atlantic in the Keathley sequence (Vogt et al., 1971). Subsequent mapping and correlation of magnetic anomalies in the Pacific revealed a concurrent sequence of correlatable anomalies on several different sets of lineations (Larson and Chase, 1972), which allowed for a world-wide correlation of M-series anomalies to be constructed and added to the GPTS, previously established for the Late Cretaceous and Cenozoic by

Heirtzler et al., (1968). Revised Mesozoic timescales primarily based on the faster spreading pacific crust were subsequently generated (Larson and Hilde, 1975; Cande 1978; Nakanishi et al., 1989), leading to the most recent revisions by Channell et al., (1995). While M-series anomalies are identified in the oldest part of the major ocean basins (e.g. Klitgord and Schouten, 1986; Vogt et al., 1971; Hayes and Rabinowitz, 1975; Cooper et al., 1976; Verhoef and Scholten, 1983; Roest et al., 1992; Sager et al., 1992; Ramana et al.,

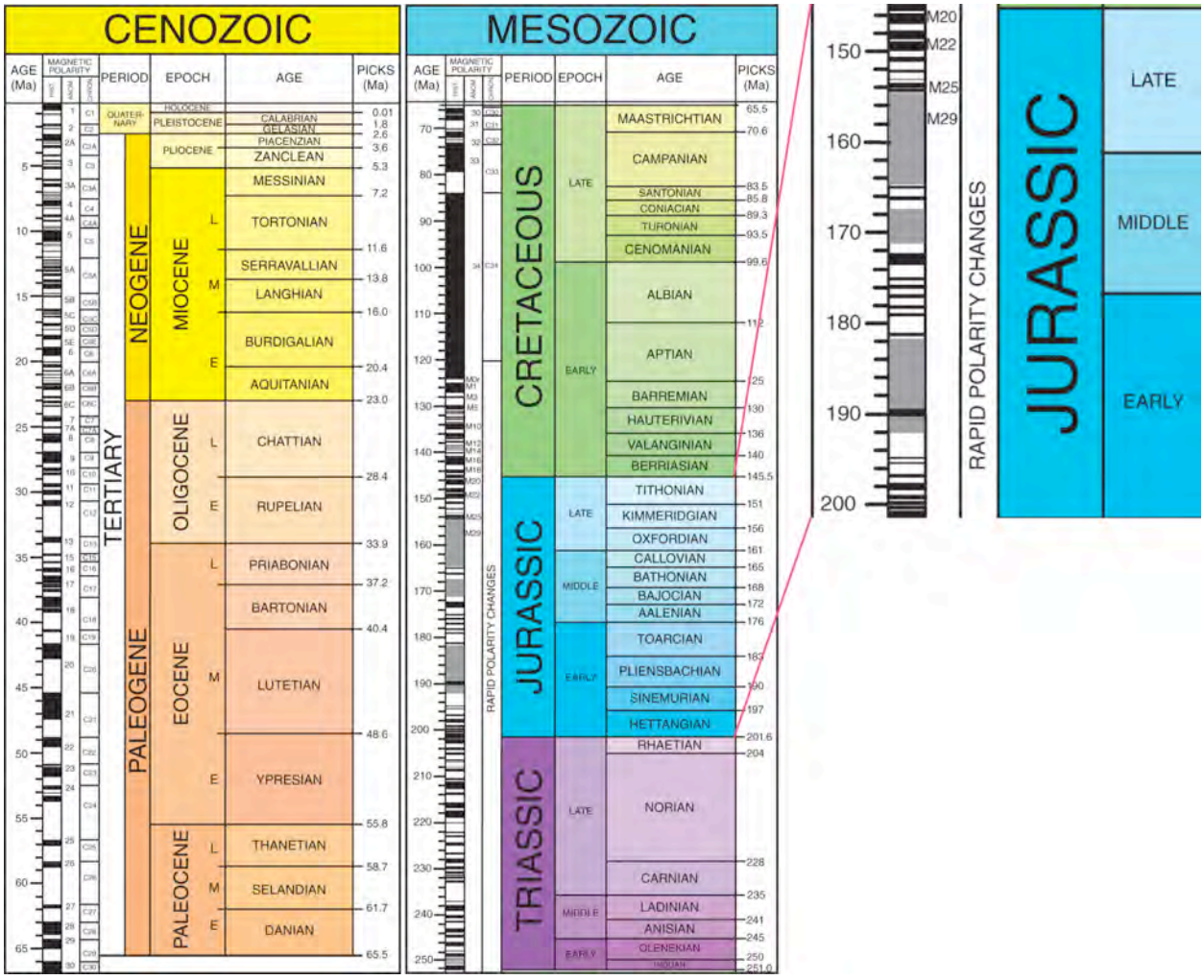

Figure 2. Geomagnetic Polarity Time Scale (GPTS) and the Geological Time Scale showing the period of time in the Jurassic that was the focus of this research cruise.

1994; Rybakov et al., 2000; Roeser et al., 2002; Ramana et al., 2001; Gurevich et al., 2006), the most complete sequence of Late- to Mid-Jurassic anomalies is only available in the western Pacific (Fig. 1). These Pacific anomalies occur as three distinct sets of lineations, the so-called Japanese, Hawaiian, and Phoenix lineations (Fig. 1) that record the early spreading history of the Pacific plate at the fast-spreading circum-Pacific ridges (Nakanishi and Winterer, 1998).

The "Jurassic Quiet Zone"

From the earliest studies of the Mesozoic anomalies (Larson and Chase, 1972) it was clear that the correlations began to breakdown around M22 time (150 Ma) as the anomalies became weaker and less distinctive. This pre-M22 period was termed the Jurassic Quiet Zone (JQZ) and considerable debate has continued as to the true nature of this period. The onset of the JQZ (Larson and Chase, 1972) was first determined based on the disappearance of correlatable anomalies in both the Atlantic and Pacific (Larson and Chase, 1972; Larson and Hilde, 1975; Cande et al., 1978; Vogt and Einwich, 1979). The younger boundary of the JQZ has changed through time as resolution has improved from M22 (Larson and Chase, 1972), to M25 (Larson and Hilde, 1975), to the present M29 age (Cande et al. 1978; Kent and Gradstein, 1985; Channell et al., 1995). The JQZ was thought to be analogous to the Cretaceous Normal Superchron (CNS) i.e., a period of single polarity but there are several lines of evidence that dispel this view. First, anomaly amplitudes monotonically decrease in amplitude from M19 toward M29 (Fig. 3, Larson and Hilde, 1975; Cande et al., 1978; McElhinny and Larson, 2003) and this decrease continues until M39 (Tivey et al., 2006), suggesting low field intensities compared to the CNS (Fig. 2A, Biggin and Thomas, 2003; Tauxe, 2006). Second, a number of efforts to investigate the pre-M29 magnetic anomalies have been undertaken in the Japanese lineations of the Pigafetta basin in the western Pacific revealing magnetic anomalies that appear to be correlatable (Handschumacher et al., 1988; Sager et al. 1998; Tivey et al., 2006; Tominaga et al., 2008). Third, terrestrial stratigraphy suggests that there were reversals during the JQZ (Steiner et al., 1986; Steiner et al., 1987; Ogg and Gutowski, 1996) and more recent results appear to confirm polarity reversals during the M25 to M38 period (Ogg et al., 2010; Przybylski et al., 2010a, 2010b). However, as anomalies become weaker in amplitude it is difficult, if not impossible, to know, whether these anomalies are the result of true polarity reversal or are simply fluctuations in field intensity (Cande and Kent, 1992; Roberts and Lewin-Harris, 2000; Bowles et al., 2003) without independent terrestrial magnetostratigraphic control. If the field is truly incoherent it may be very difficult for even magnetostratigraphy to verify field behavior and global correlation becomes an important factor. Regardless of their cause, however, if a magnetic anomaly can be correlated globally then it is still useful as a time marker.

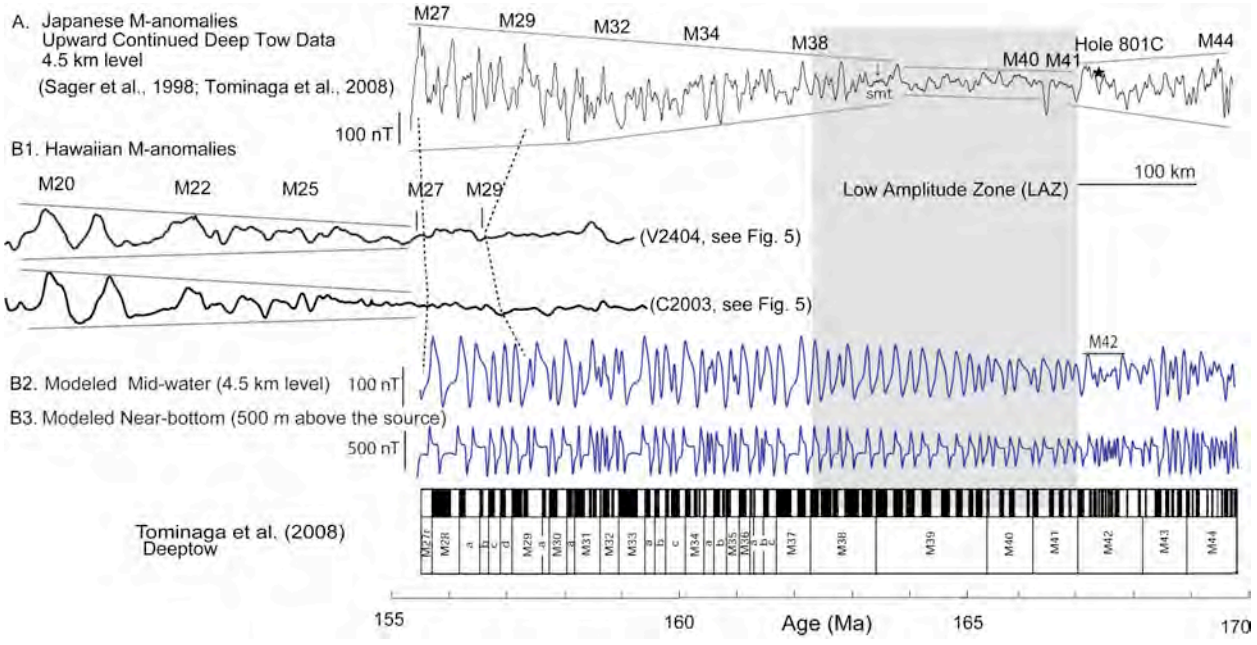

Figure 3. Summary of previous sea surface and deeptow magnetic profiles in the Pacific Jurassic region A) shows upward continued Japanese deeptow magnetic profile, B) shows the sea surface magnetic profiles from Larson and Hilde (1975). Bottom panel shows modeled deeptow magnetic sequence from the Japanese lineations (Tominaga et al., 2008)

Recent Results from the Japanese Jurassic Crust

Early studies could not resolve pre-M29 magnetic anomalies (>157 Ma) by surface-towed magnetometer because of the reasons mentioned above (Fig. 3). To overcome the diurnal noise issue, Handschumacher et al. (1988) conducted an aeromagnetic survey over the Japanese lineations of Pigafetta basin and found correlatable anomalies from M29 to M38 (162.5 Ma). Two deep-tow magnetic surveys were subsequently conducted in the same region of the Pacific Japanese lineations (Sager et al., 1998; Tivey et al., 2006; Tominaga et al., 2008). Deep-tow surveys can overcome the signal-to-noise issue because the magnetic sensor is towed near the seafloor and recovers the maximum amplitude and spatial resolution without suffering the distance from source attenuation and lateral smoothing inherent in surface towed measurements (Fig. 3A). Sager et al. (1998) collected two 800-km-long deep-tow magnetic profiles that extended the correlations of Handschumacher et al (1988) from M38 to M41 (167 Ma). A second deep-tow magnetic survey (Tominaga et al., 2008) extended the correlations to M44 (170 Ma). These deep-tow data reveal that magnetic anomalies are present throughout the time period from M38 to M44 (Tominaga et al., 2008). Anomaly amplitudes decrease to about M39, which marks the onset of a confused period of low amplitude anomalies that are difficult to correlate – the low amplitude zone or LAZ. Prior to the LAZ, correlatable anomalies reappear and become stronger in amplitude starting at M42 (167 Ma) and continue to M44 (ca. 170 Ma). Chron M42 provides a tie with downhole magnetization logs and samples of ODP Hole 801C that strongly suggest that polarity reversals are present, consistent with the overlying anomaly

sequence (Steiner et al., 2001; Tivey et al., 2005). Chron M44 marks the transition from rough to smooth (RS) basement topography and is thought to mark the limit of pristine Jurassic-aged crust and the appearance of Cretaceous sills overlying and intruding Jurassic basement (Abrams et al., 1993). M44 may mark the edge of a Cretaceous volcanic province overprint (Abrams et al., 1993) or it may be a fossil plate boundary, a fracture zone trace, or mark a change in spreading rate or direction (Handschumacher et al., 1988). The deeptow magnetic data also suggest that reversal rate is high during this pre-M29 period assuming that all anomalies are caused by polarity reversals. Even if we discount the low amplitude anomalies in the LAZ, we still calculate reversal rates of 10 rev/My, which is very fast compared to Cenozoic rates of 0 to 5 rev/My (Opdyke and Channell, 1996; Tivey et al., 2006). These results are problematical when we seek to expand their significance to more global proportions. For example, we have made correlations on only two profiles from one part of the Pacific basin and so we need confirmation from a separate record formed at a different midocean ridge spreading center to verify that these correlations are more global in their significance, i.e., geomagnetic in origin. Similarly, we have found a zone of poor correlation with low amplitude anomalies (the LAZ), but we cannot tell if this is due to local tectonics or crustal contamination from later stage volcanics or it truly reflects geomagnetic field behavior. Only by surveying the same age crust that has formed at a different mid-ocean ridge spreading center can we begin to make a case for the global significance of these observations.

We have some hope that some of these observations are supported by independent observations. In the Atlantic, Roeser et al. (2002) presented the correlations of Atlantic pre-M29 anomalies to M41. Although hampered by the slow spreading regime, the Atlantic work gives hope that the existence of correlatable pre-M29 anomalies is verifiable in a global context. Confirmation that these pre-M29 anomalies are truly polarity reversals is also beginning to be supported by terrestrial magnetostratigraphic work. A compilation from Mesozoic Tethys sections clearly shows clear pre-M29 reversals back to M38 (Ogg et al., 2010; Przybylski et al., 2010a, 2010b). We do not have any corroboration of the LAZ at the present time, which more than any other result appears to be the most confounding observation of Jurassic Earth's magnetic field so far.

Cruise Objectives

Our overarching hypothesis is: The geomagnetic field during the Jurassic was behaving in a globally coherent way.

If we can confirm the global coherency of field behavior, we will be able to define a unique style of field behavior, the LAZ, that appears to be the antithesis of the CNS. We will also be able to build a foundation for a better Late- to Mid-Jurassic GPTS extending the timescale to approximately M44 (~170 Ma). Even if we cannot correlate between the Japanese and Hawaiian JQZ anomalies, we still have important information about Earth's geomagnetic field and advance both numerical and laboratory modeling of field behavior. More specific questions that we can address with our proposed field program are as follows:

(1) Is the M29-M38 anomaly sequence measured on the Japanese lineations characteristic of field behavior during this period?
The deep-tow results from the Japanese lineations (Tivey et al., 2006; Tominaga et al., 2008) reveal a decreasing anomaly intensity and variations in reversal rate over the M29-M38 period. A new Hawaiian Jurassic seafloor magnetic record would allow us to confirm and refine a geomagnetic polarity time scale (GPTS) for this period with more confidence. It would help the ongoing terrestrial magnetostratigraphy efforts by proving a broader context for their results.

(2) What is nature and origin of the LAZ (M39 to M41 anomalies)
Results from surveys of the Japanese lineations (Tivey et al., 2006; Tominaga et al., 2008) reveal a period when magnetic anomalies are weak and apparently incoherent – the LAZ. It is important to identify if the LAZ is a local phenomenon due to tectonic or crustal influences or if it truly is representative of geomagnetic field behavior. By measuring the magnetic record for this period at a different spreading center we will be able to either verify or eliminate any local tectonic or crustal variations as a source of the LAZ. Our seismic results should also allow for better characterization of tectonic and crustal effects.

(3) Does M44 mark the end of the marine magnetic Jurassic record?
We do not know if M44 is the oldest identifiable marine magnetic record based solely on the data from the Japanese Jurassic seafloor. It also marks the onset of rough-to-smooth basement topography (Abrams et al., 1993). Both our magnetic and seismic data should help to verify if this zone also occurs on the Hawaiian lineation sequence and at the same time period. If the M42-M44 anomalies can be verified, it may be possible to extend the magnetic record beyond the M44 chron. The older we extend our correlation of the marine magnetic record, the better we will constrain the birth of the Pacific plate in time and space.

In addition to addressing questions about Jurassic field behavior, we expect a key deliverable will be a more robust and improved geomagnetic polarity time scale (GPTS) model for the Mid-Jurassic. When one looks at a commonly available Geological Time Scale, such as the recently published Geological Society of America (GSA) Time Scale (Walker and Geissmann et al., 2009), it is immediately obvious that the GPTS begins to break down in the Jurassic (145 to 201 My) period, typically around the M25-M29 chrons, the last presently accepted magnetic chron of the GPTS (Fig. 2).

Overall Operation Plan

During our 42-day cruise (including 10 days transit), we collect high-resolution near-bottom magnetic data over the Late- to Mid-Jurassic section of ocean crust in the Hawaiian magnetic anomaly sequence of the central western Pacific. We use the Autonomous Underwater Vehicle (AUV) Sentry operated by the National Deep Submergence Facility (NDSF) to collect pre-M29 near-bottom magnetic anomalies on the Hawaiian portion of the Pacific JQZ. These magnetic profiles will provide an opportunity to correlate between the Hawaiian pre-M29 anomalies and the Japanese lineations to construct an accurate Geomagnetic Polarity Time Scale (GPTS) model that is more representative of global

magnetic field behavior. We also collect multi-channel seismic reflection and refraction data during the cruise on times the AUV is recharging its batteries. These seismic data allow us to image depth to basement and Jurassic crustal structure and to evaluate whether the crust has been affected by intra-plate volcanism that is widespread in the western Pacific (e.g. Schlanger et al., 1981; Abrams et al., 1993; Tarduno et al., 2001).

Exposure to the Field Oceanography

Throughout our field program, we will advance discovery while promoting teaching and training by providing at-sea research experience for several graduate and undergraduate students. In particular, PIs from WHOI and Kutztown University of Pennsylvania will enhance infrastructure for research and education by establishing collaborations with students and faculties between research (WHOI) and teaching (Kutztown) institutions through the proposed research.

TN272 Preliminary Results

Overall Achievements

We sailed on the *R/V Thomas G. Thompson* (TN272 Cruise) in November-December 2011, to carry out the proposed survey plan (Fig. 4). The cruise departed from Honolulu on Nov 5th and transited to a spreading corridor we had identified in the Waghenaer fracture zone region [Mammerickx and Smith, 1985; Nakanishi et al., 1989] (Fig. 1). Here, we picked up the first M19 anomaly sequence as our tie and then surveyed along the corridor, south to the M28-M29 anomaly sequence, where we initiated the near-bottom survey program. The cruise returned to Guam on Dec 17th.

Briefly, we were able to obtain the following basic results:

1) More than 9,000 km of surface-towed total magnetic field data between Hawaii and Guam.
2) Approx. 770 km of mid-water towed (3.5 km depth) MISO TowMag magnetics
3) Complete MCS coverage along the 800 km corridor – including 49 sonobuoy refraction records.
4) Ship-based EM302 30 kHz multibeam and 3.5 kHz chirp subbottom sonar along with shipboard gravity data
5) Two 60 km survey transects with AUV Sentry. We had one other dive with a small amount of data collected. The 5 remaining dives were either test dives or were not successful.

While we can claim success in several aspects of the cruise, the most critical component of the cruise failed, which was the collection of near-bottom AUV Sentry magnetic data. Only two complete Sentry dives of 60 km each for a total of 120 km (note the profiles are not contiguous) (Fig. 4) were obtained out of the planned 800 km corridor i.e. only ~20% of the planned program.

General Cruise Operation and Logistics

The RV Thomas G Thompson left Honolulu, HI at 9:15 AM, November 5th 2011 to the investigation of the nature of Jurassic geomagnetic field recorded by Hawaiian Jurassic crust. We first stopped at around 2000 m water depth near Oahu Island to conduct USBL calibration. We then proceeded to the 6000 m water depth to conduct Sentry dunk test (Sentry dive 127). After the completion of the dunk test, we had a long transit to the survey site (Nov. 7th -12th). While this transit, we deployed surface-towed magnetometer to assess juxtapositions of previously identified M-series anomalies. Nov. 14th, we confidently located ourselves at M19-M29 areas by multiple survey lines. Nov. 15th, the first seismic operation started. After ~ 60 km of seismic survey completed, we deployed USBL pole and TowCam to support the first Sentry dive (dive 128). The recovery mission lasted for a couple of hours toward the dawn of Nov. 17th. We immediately conducted the operation

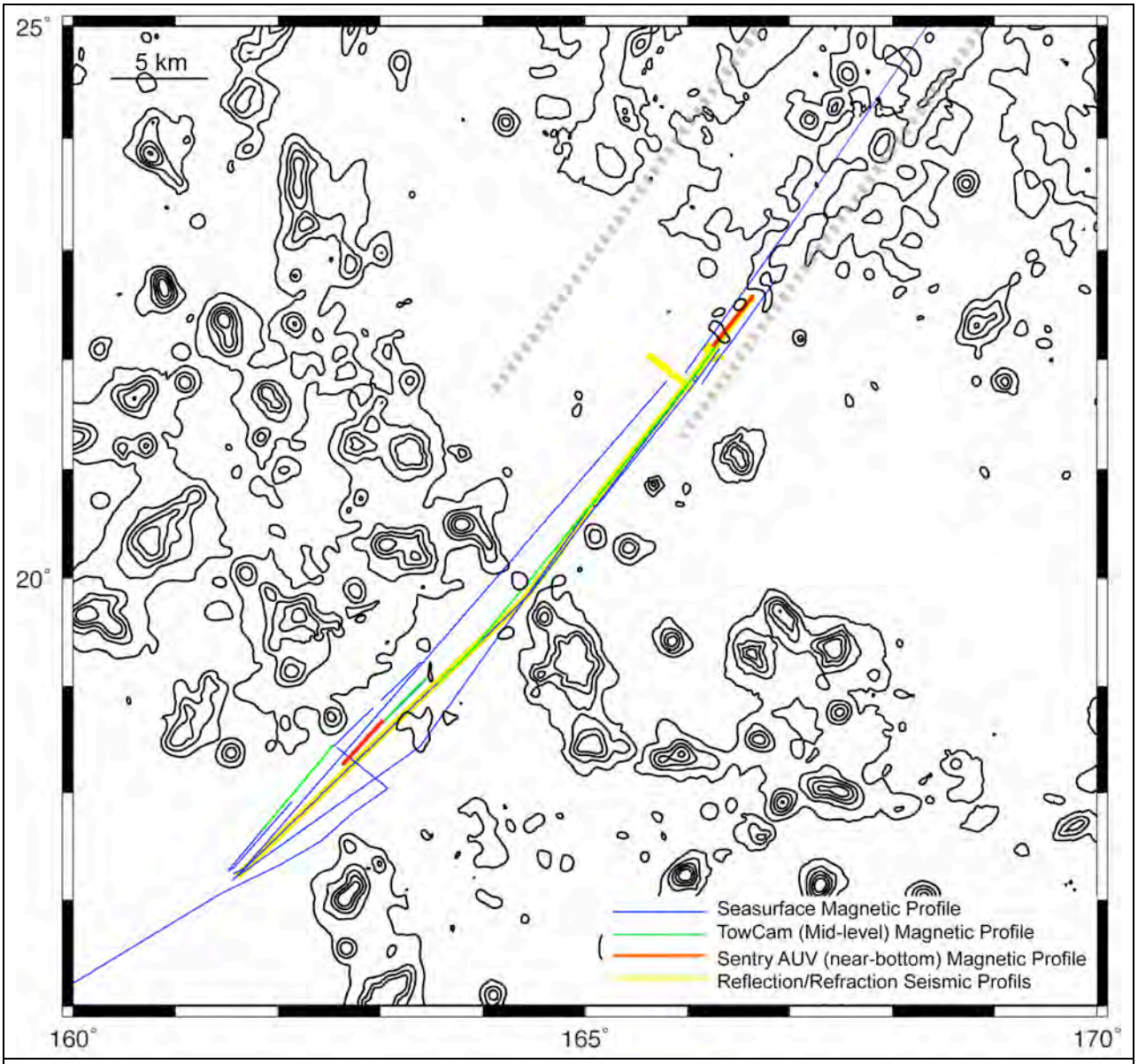

Figure 4. Trackline map of TN272 showing sea surface profiles (blue), Mid-tow TowCam (green) and two successful Sentry profiles (red). Yellow lines show seismic coverage.

with seismic. We conducted long seismic survey line (seismic Line #2) to extend our survey profile further SW. Nov. 18-19th, due to the weather (cold front passing through and mixed/combined sea of >15 ft swells), TowCam test, supported by the Captain, manifested that this sea condition was not safe enough to use the hydroboom (and the test resulted in terminating a short amount of CTD cable). As a weather contingency, we deployed surface towed magnetometer and proceed to the end of designated survey line and back to the end of Seismic line #2. Nov. 21st, we shoot seismic cross line to investigate segment-wide distribution of sills. Sentry dive 129 was conducted afterwards. In dawn of Nov. 23rd, Sentry's extensive search mission was conducted for a total 4 hours. While providing

significant information for the AUV engineering, this search mission consumed extra science time due to the difficulty in tracking the vehicle underwater, indicating the severe limitation of Sentry operation in ~ 6000 m water depth. After we recovered Sentry, we conducted the second seismic cross-section shooting to characterize the distribution and character of possible Cretaceous sills observed from sonobuoy data. Nov 23-26th, we carried out a long mid-water level magnetic survey by TowCam to prioritize extending our magnetic profile. At the completion of the TowCam survey, we conducted Sentry test dive to investigate the functionality of forward actuator (Sentry Dive 130). The dive was unsuccessful due to the programming error. Subsequently, we conducted 303 nm seismic survey line to finalize our investigation of the crustal nature of the magnetic source to the end of ~ 800 km line to dedicate the rest of our ship time for magnetic survey including Sentry operations. This seismic operation lasted until Nov. 30th and we successfully completed all our proposed reflection and refraction seismic operations. After we secured the seismic gears on deck, we conducted Sentry shallow-dive test (second try). The sea state of the night of Nov. 30th was moderate, combined sea where swell and wind directions were hard to detect at first hand. Sentry AUV recovery mission turned into a major challenge for both ship and AUV crews. Sentry AUV broken its starboard wings from this recovery mission. While Sentry was under repair, we deployed the surface-towed magnetometer to fill the data gap in the ~ 800 km line, particularly within "The Lost World" site where low amplitude anomalies from the previous tows need to be confirmed. Dec. 2nd, after we reached the end of the surface magnetometer line, we conducted a short Sentry deep dive test for 10 hours (Dive132). The recovery mission in the early Dec. 3rd morning was swift and graceful, with still a room for improvement. After we secured the Sentry on deck, we deployed TowCam back in the water to obtain a long mid-water towed magnetometer profile for the 303 nm seismic line. This TowCam run was operated with two-battery system to minimize deployment/recovery time for battery changes (Dec. 6th after 80 hrs 14 min.). TowCam survey continued until 19 degree N, then we haul in the TowCam, conducted multibeam survey to map the uncharted terrain where next Sentry dive with TowCam operations are anticipated. We deployed Sentry 12:17 local on Dec. 7th (Dive 133). After successful Dive 133, we towed surface magnetometer and map the uncharted terrain. The weather of Dec. 8th was, however, not good enough for Sentry dive (particularly recovery). Thus, we extended the survey line for TowCam operation to maximize the coverage by mid-water magnetic profiles. At the noon of 13th, we recovered TowCam on deck, and deploy the surface-towed magnetometer for the last part of the science operation. We extended the surface-towed magnetic profile to confirm the M41-42 anomalies. We crossed the old Pacific "forgotten triangle" to WSW further extending this surface magnetic line. After we crossed Marianas Trench, we haul in the surface-towed magnetometer; then, only multibeam and chirp sonar were ran until we arrive at Guam.

3. Near-bottom Magnetics—Sentry Autonomous Underwater Vehicle

Our cruise was designed around collecting the highest resolution magnetic data using the Autonomous Underwater Vehicle (AUV) Sentry (Fig. 5). Sentry is the new AUV that replaced ABE in the National Deep Submergence Facility (NDSF) in 2009. Sentry is a tetherless vehicle that navigates independently from any surface vessel using its onboard doppler velocity log sonar (DVL) and inertial navigational system (PHINS). Prior to our cruise, Sentry was fitted with three, 3-axis APS fluxgate magnetometer sensors (Fig. 5)

arranged in both a horizontal (mag0 and mag1) and vertical (mag2) gradiometer mode. Along with the magnetometers,

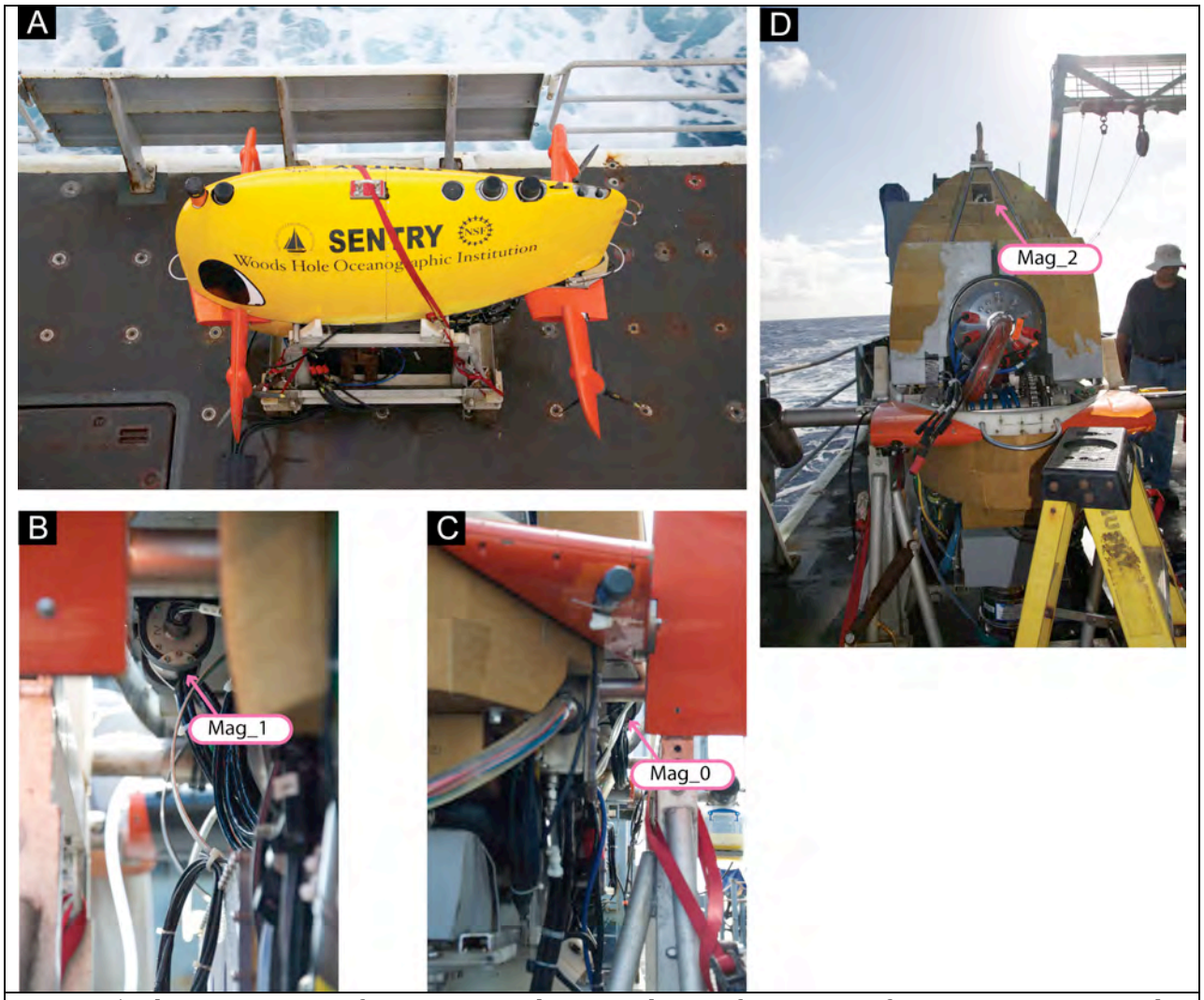

Figure 5. Photo montage of AUV Sentry showing the configuration of magnetometers on the vehicle. Two are mid-ships port and starboard and one is in the top of the body.

Sentry also carries a depth sensor, altimeter, CTD and a chirp subbottom sonar. This instrument/acquisition configuration was chosen to extend the battery life as long as possible for each dive operation. We chose not to use the Reson multibeam or sidescan capabilities as we did not expect to have any significant bathymetric features or seafloor structures along the transect.

Onboard the TN272 cruise, we only pre-processed the data acquired by the mag-2 magnetometer because of noises appeared in the mag-0 and mag-1 data. The source of the noises is likely a capacitant-induced electric current, probably due to the actuator of the vehicle. The mag-2 magnetic data are vector field with the accuracy of ±2 nT. We calibrated

the vector data to the vehicle motion using Korenaga (1995) routine; then, we used the motion-calibrated total field data for the upward continuation (Guspi, 1987) to plot against mid-water data and sea-surface level data in checking the data quality.

Because of AUV Sentry system problems, we were only able to obtain data on two dives (128, 134) during the cruise, however, these two dives highlight the key motivation for why such near-bottom data are of critical importance to our originally proposed research. The water depth in this part of the western Pacific is nominally > 5500 m, thus magnetic anomalies obtained by surface-towed magnetometer and even at the mid-water (~3-4 km depth) level (TowMag) are significantly attenuated in anomaly character and amplitude (Fig. 6). Diurnal variations are more enhanced at equatorial latitudes so that small amplitude signals, at the sea surface in particular, are also likely to obscured by non-geologic issues. Furthermore, Late- to Mid-Jurassic magnetic anomalies are thought to be a combination of small amplitude and short wavelengths, which are difficult to detect by surface-towed or mid-water level profiling (Tivey et al., 2006; Tominaga et al, 2008). As Figure 6 shows, the mid-water level profiles (TowMag) are useful but lack the detailed

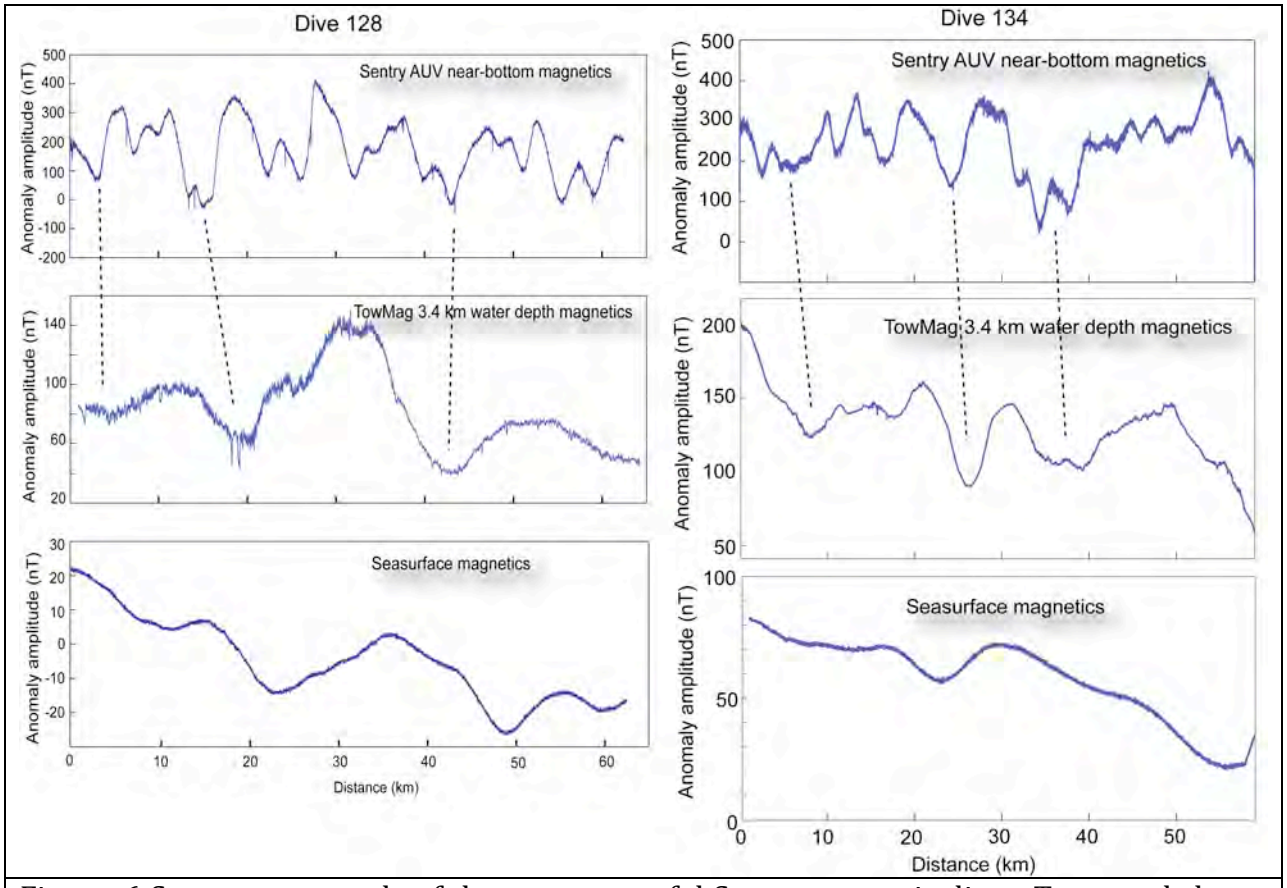

Figure. 6 Summary example of the two successful Sentry magnetic dives. Top panel shows the sea surface magnetic profile, mid panel shows the mid-tow TowMag profiles, and the bottom panels show the Sentry magnetic profiles.

structure that is obviously apparent in the Sentry bottom profile (Fig. 6). The near-bottom magnetic data obtained by the Sentry AUV images the most detailed magnetic anomaly record yet available in the Jurassic ocean floor, in which short–wavelength anomalies are clearly and unambiguously defined compared to the concurrent mid-water resolution profile.

4. Mid-water Magnetics - TowCam Magnetometer Sled

To augment the AUV Sentry operations and to provide a backup in case of technical problems we used a deeptowed sled provided by the WHOI-MISO facility. Instead of the usual complement of deep sea cameras we installed two magnetometer sensor systems, a pressure depth sensor and an SDSL (Subsea Digital Subscriber Link: ref. Swartz) communication interface to provide real-time data up the CTD 0.322 conducting cable to the ship. The University of Washington Shipboard Operations Group had a Marine Magnetics SeaSpy Overhauser magnetometer designed to be towed at depths up to 6000 m off of the 0.680 conducting sea cable. In discussion with the UW Shipboard Operations Group and Dan Fornari of MISO we decided to utilize this system on the Towcam sled as part of the deeptowed magnetometer configuration. The SeaSpy was mounted on in sled which is constructed of non-magnetic aluminum framing (Fig. 7). A small Honeywell HMR2300 digital magnetoresistor 3-axis magnetometer sensor was also mounted on the sled fin. A SeaBird pressure sensor model SBE 52 rated to 7000 m was mounted on the sled frame to provide depth information. Power was supplied by a rechargeable 24V 42 amp/hr Deep Sea Power and Light lead-acid battery mounted forward on the Towcam frame. Each of the sensors (Seaspy, HMR minimag and SeaBird depth sensor) provides an RS-232 data stream which is sent to a central SDSL bottle containing MOXA N-port convertors that translate these signals into Ethernet packets that are then transmitted up the CTD cable to the surface ship side using the SDSL protocol. The CTD wire termination at the sled used the red and white conductors only, which were connected to the SDSL output pigtail cable consisting of two wires (also red and white). The remaining CTD black conductor was left unconnected and was left to float with respect to armor (it cannot be paralleled with another conductor or tied to ground). No seawater return on the armor is used for the data link and no power is sent down the cable. The output of the SDSL Data Link is an AC signal with no polarity and so wiring can be switched with no effect. Topside, the two wires from the CTD wire come into the TGT Computer Lab rack to a terminal barrier block and then to an Ethernet cable that is connected to logging laptop running Ubuntu and logging software provided by James Kinsey and Stefano Suman of the Sentry group.

Summary of TowCam SDSL connections:
J1 sea cable
J2 power
J3 SeaSpy
J4 HMR minimag
J5 SBE50
J6 n/c (but reconfigured during cruise to connect to AVTrak USBL)

Serial Interfaces on J4-J6

Moxa "J4" 128.128.22.36
P1: HMR minimag 9600,n,8,1 (HMR configured to "spit data"
P2: n/c

Moxa "J5" 128.128.21.207
P1: SBE50 9600,n,8,1

P2 n/c

Moxa "J6" 128.128.22.37
P1: SeaSpy deck unit inside SDSL, 9600,n,8,1
P2: n/c

Cables
VMG4FS -> MCIL6F HMR minimag
1-1, 2-3, 3-6, 4-2, 4 n/c, 5 n/c

The logging software time stamped the incoming data streams and flagged the data source as shown in the snippet below.

MMD 2011/12/02 17:36:24.677 SRC_TMG_MMD *10.046/01:16:00.5 F:009043.067 S:073 D:+000.0m A:035.38m L0 0465ms Q:49

HMR 2011/12/02 17:36:24.680 SRC_TMG_HMR 4,609 903 684
HMR 2011/12/02 17:36:24.783 SRC_TMG_HMR 4,609 901 685
TSD 2011/12/02 17:36:24.870 SRC_TMG_TSD 0.26

MMD indicates the SeaSpy magnetic data and was generally setup to cycle at 1 Hz. HMR indicates the HMR minimag sensor output in raw millivolts and is at a 10 Hz rate. TSD indicates the SeaBird depth output in meters running at approx. 5 Hz. Log files are made every hour (20111202_1736.GEF) with a date string as filename. A perl script parses these files for input into MATLAB for further processing. The HMR minimag millivolt output is converted to nanotesla by multiplying by 6.667 nT per millivolt.

The first 6 dives utilized a single battery option. Tows 3,4,5 were continuous and took the batteries to their limit in terms of duration. The battery drain was significantly increased by adding an AVTrak unit to the SDSL unit in order to better track Sentry. After it was clear that TowCam tows would need to be done on a longer time basis due to difficulties with Sentry we reconfigured the sled after tow #6 to use a double battery set up. A battery harness with batteries in parallel was fabricated. This resulted in longer tows. Without using the Avtrak the tow times increased significantly. For example, for Tow 7 had an 80 hour 35 min single deployment.

We successfully obtained mid-water towed magnetic data at the 3.5 km depth level using the MISO TowMag sled over the entire 800 km transect. The original plan was for the TowMag and AUV Sentry to be operated simultaneously with the TowMag providing additional navigational capability for the Sentry vehicle. Unfortunately, because of the

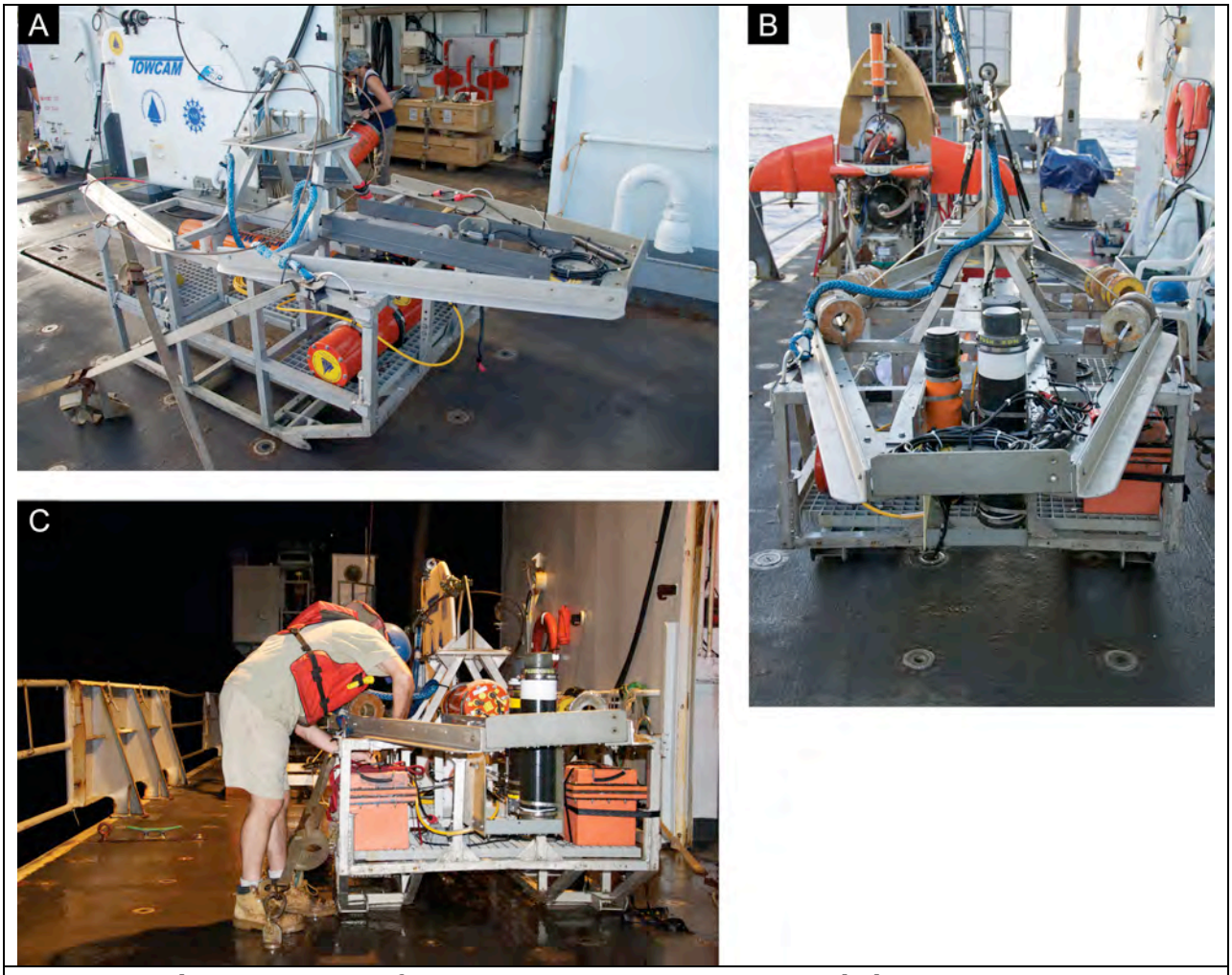

Figure 7. Photo montage of MISO TowCam Magnetometer sled. Two magnetic sensors were used on the sled. A Univ. of Washington supplied deeptow version of the Marine Magnetics seaspy overhauser magnetometer (orange sensor body) and a 3-axis vector HMR2300 magnetometer. The digital data were sent up the CTD cable in realtime using a SDSL link.

problems with the Sentry this simultaneous operation was only obtained on a couple of dives. A total of 12 tows were completed covering approximately 770 km, almost the entire 800 km transect (Fig. 4, Table 2). The TowMag was equipped with a total field Overhauser SeaSpy magnetometer and a 3-axis vector magnetometer as well as a depth sensor. These data were sent over the CTD wire to the ship in real-time using an SDSL link. While the TowMag collected excellent data for a towed body there are a number of drawbacks with this kind of deep-towed system.

The mid-water level magnetic anomaly data collected by TowMag confirms several of the details inferred from the sea surface anomalies (Fig. 8). The mid-water anomaly pattern shows long wavelength variations compatible with the anomalies seen at the sea surface

and shorter wavelength variations that point to a relatively rapid reversal rate as seen in the Japanese deep-tow anomalies. Again, more analysis work needs to be done to correct the midwater data for tow sled depth variation and to join individual tows together before a complete interpretation can be advanced. While the TowMag collected excellent data for a towed body there are a number of drawbacks with this kind of deep-towed system.

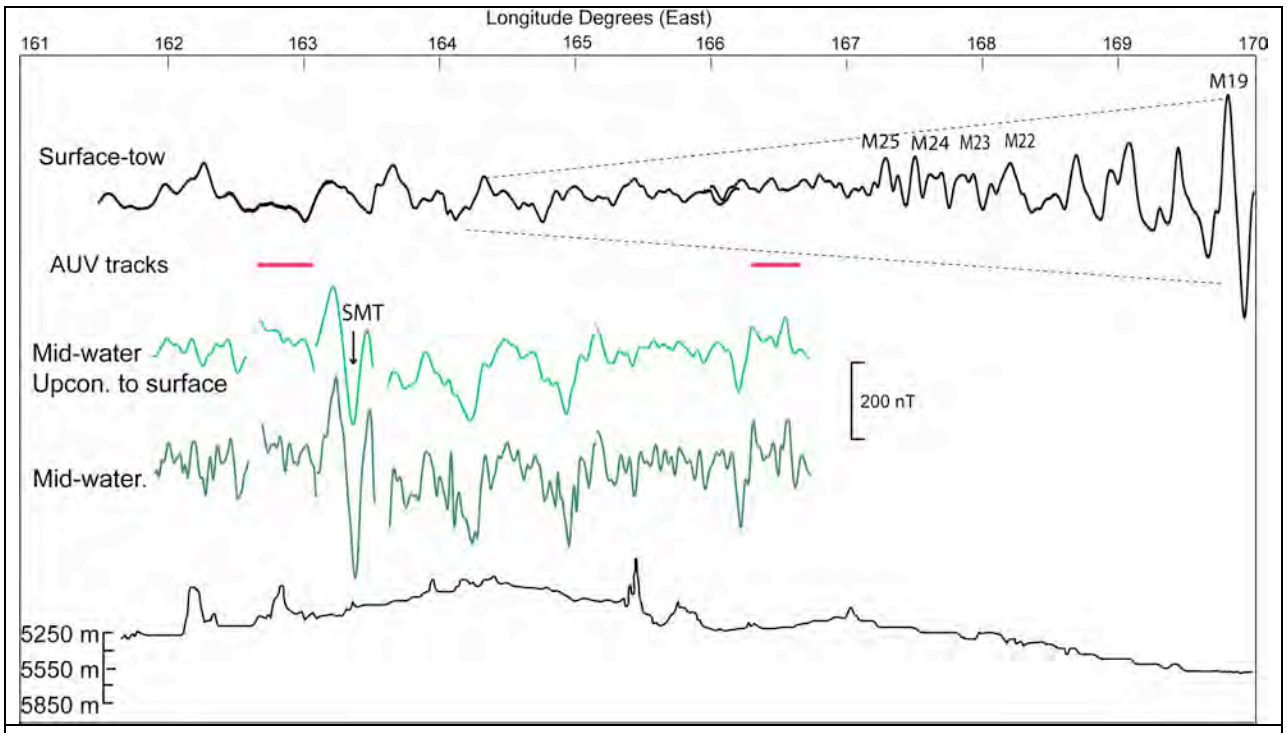

Figure 8. Summary profile of midwater TowCam Mag profiles in comparison to sea surface profile and the seafloor bathymetry.

5. Surface-level Magnetics - Sea Surface Magnetometer

A Marine Magnetics Seaspy marine magnetometer was used collect sea surface magnetic measurements during the cruise. The magnetometer was deployed from a small special-purpose air-tugger winch on the port side of the fantail. Both the winch and magnetometer (Fig. 9) were supplied by the WHOI-MISO facility. The magnetometer cable was 300 m in length (approximately 13 m on deck with the remainder deployed over the rail). A coaxial conductor deck cable (100 m) ran on the port side of the ship through the Hydrolab into the Computer lab. The Seaspy magnetometer is an Overhauser nuclear precession type of sensor that collects total field data at a fast rate (typically for this cruise 1 sec rep rate) with a reported accuracy of 0.1 nT. Data from the magnetometer were logged directly into the ship's logging system and recorded using the Marine Magnetics SeaLink software (ver. 8.00046), and synchronized with the ship's P-code #1 GPS navigation feed. Time was manually set to GMT. The magnetometer was used during most transits at speeds of up to 14.3 kts at times. Neither the integrity of the cable and sensor

bottle or data quality suffered from this tow speed. The built-in depth sensor was mostly unreliable, but other than that, the magnetometer performed flawlessly. We purposely did not attempt to tow the magnetometer during slower seismic operations (4kts) or deeptow operations (1.5 kts). Sea surface magnetic profile times are listed in Table 2. A map of tracks and the anomalies are shown in Figs. 4 and 10.

Figure 9. Photo of WHOI-MISO Sea surface towed Marine magnetics Seaspy magnetometer system.

We collected just over 9000 km of high quality sea surface magnetic data in order to provide a robust tie in with existing timescale and magnetic anomaly identifications [Larson and Hilde, 1975; Cande et al, 1978; Nakanishi et al., 1989] and to provide the overall context for the new near bottom magnetic data we planned to collect. It was our contention that a Jurassic spreading corridor existed between the North and South Waghenaer fracture zones (the extension of the Mendocino fracture zone) that extended across the Marcus-Wake seamount chain into the Pigafetta basin (Fig. 3). We were able to tie the northern end of the survey line to the M19 chron and confirm progressively older anomaly identifications up to the M29 chron [Nakanishi et al., 1989], the last currently acknowledged GPTS chron in the marine timescale. The M29/M28 chron was used as the tie point and beginning of the 800 km long near-bottom magnetic transect (Figs. 4 and 5). We collected sea surface magnetic data along this entire transect and deep into the Pigafetta basin crust and made sure we collected multiple parallel profiles so as to confirm lateral variability of lineations and to minimize the magnetic effects of late-Cretaceous seamounts.

The sea surface data show the overall decrease in anomaly amplitude from M19 to M29 (Fig. 10), followed by a period of low amplitude, which in turn is preceded by a return to stronger amplitude anomalies. As the profiles cross into the Marcus seamount chain there are a few anomalies contaminated by seamount effects, but we can interpret basic patterns that suggest a lineated set of anomalies is present. This pattern is very similar to our Japanese anomaly sequence but it is too early to say (the TN272 cruise was completed on December 17th, 2011) if the timing can be related to the same LAZ we see in the Japanese lineations. More work will need to be done to fully process and model these anomaly records, but we feel confident that a robust interpretation is attainable.

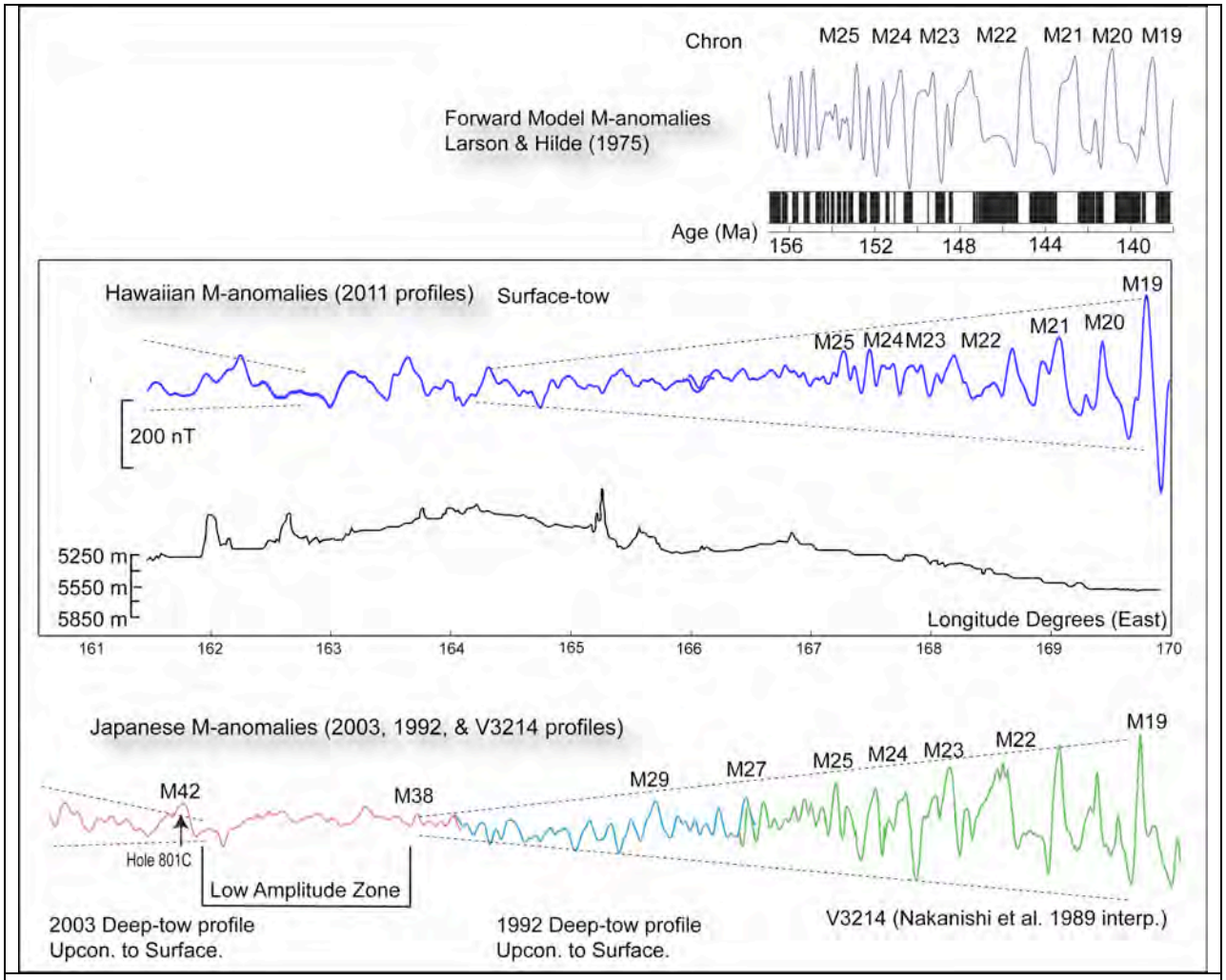

Figure 10. Summary of collected sea surface magnetic profiles in comparison with previous profiles.

6. Shipboard Systems

Navigation systems and Data Acquisition System

The RV Thompson has six Global Positioning System (GPS) receivers that are used for various tasks. The C&C Technologies C-NAV World D-GPS receiver is the primary navigation source for the cruise and is used as the primary source for the DAS data display system. The second GPS unit is the POS-MV, which is the primary unit used for the EM302 multibeam system. The POS-MV also has a C-NAV feed to provide a backup GPS source. The ship also has two P-code GPS receivers primarily used as backup. The WinFrog navigation used by the Dynamic Positioning system uses all four of these navigation sources. The bridge also has a Furuno GPS source for navigation that is not available for science use. Finally, a sixth GPS source is used by the "wind" sensor computer. We experienced several short periods of occasional GPS signal loss from one or more of these GPS sources during the cruise.

The DAS (Data Acquisition System) is an informational display that records basic shipboard data every 5 seconds and writes to a file on the data-share drive as TN272DAS.julian_day. The format of the files are ASCII comma separated values that can easily be imported into Excel, Matlab or ArcGIS (see below for the listing of values). Although an averaging of the lat/lon values is implemented, occasional "flyers" of bad navigational data do make it into the data files. We also secured the ship's shallow ADCP so that ship's Doppler Speed Log was inoperative and gave a fixed value of 9.7 kts for the duration of the cruise. As mentioned the CNAV GPS is the primary navigational source for the data with POS-MV as a backup. The depth recorded by DAS is the EM302 multibeam depth when that system is operating or when the EM302 is secured, the Chirp 3260 depth. During the cruise there were periods when we turned off both the EM302 and Chirp 3260 for Sentry operations and consequently no depth is recorded by the DAS system.

The file configuration for DAS files TN272DAS.XXX follows:

Value 1 = Nav computer GMT date (dd/mm/yyyy)
Value 2 = Nav computer GMT time (hh:mm:ss)
Value 3 = Nav computer latitude (+/-dd.dddddd)
Value 4 = Nav computer longitude (+/-ddd.dddddd)
Value 5 = Gyro compass heading (degrees true)
Value 6 = Nav computer COG (degrees true)
Value 7 = Doppler speed log (knots)
Value 8 = Nav computer SOG (knots)
Value 9 = Thermosalinograph temperature (degrees C)
Value 10 = Thermosalinograph external sea temperature (degrees C)
Value 11 = Thermosalinograph conductivity (Seimens/meter)
Value 12 = Thermosalinograph salinity (PSU)
Value 13 = Thermosalinograph chlorophyll (volts)
Value 14 = Thermosalinograph light transmission (volts)
Value 15 = Water Depth (meters)
Value 16 = IMET air temperature (degrees C)
Value 17 = IMET relative humidity (percent)
Value 18 = IMET barometric pressure (millibars)
Value 19 = PAR (microEinsteins per square meter per second)
Value 20 = IMET short wave radiation (watts/square meter)
Value 21 = Wind speed true (knots)

Value 22 = Wind direction true (degrees)
Value 23 = Wind speed relative (knots)
Value 24 = Wind direction relative (degrees)
Value 25 = Average true wind speed (knots)
Value 26 = Average true wind direction (degrees)
Value 27 = Sound Velocity (meters/second)
Value 28 = Winch ID number (see note below)
Value 29 = Wire out (meters)
Value 30 = Wire rate (meters/minute)
Value 31 = Wire tension (lbs.)

Winch ID. =
0 = Hydro Winch 1
1 = Trawl Winch
2 = Hydro Winch 2

EM302 Multibeam Bathymetry

The R/V Thompson has a Kongsberg Simrad EM302 sonar. While the EM 302 is a high frequency (30 kHz) multibeam that is designed for optimum performance in water depths shallower than ~3000 m, we used it throughout this cruise in "extra deep" ping mode for the 5000-6000 m depths of our survey region. Full beam swaths widths varied between 4000 m and 10,000 m or more depending on the angle settings for the beams generally 15 to 36 degrees. The system has 432 beams and we utilized the high density equal distance mode for the distribution of the beams. Dual swath mode was turned off and pitch stabilization was turned on. The POS-MV provided yaw stabilization information. Sound speed information was obtained from periodic XBT measurements. The grid cell of the graphic displays was set to 60 m cell size on a Mercator-WGS84 projection. The system had various panels where filters could be turned on or off depending on the conditions of the environment. Generally, the seafloor in the survey area was flat and averaged around 5000 to 6000 meters. Typical filtering settings utilized a "medium" Spike Filter Strength, "small" Range Gate, "normal" Phase Compensation, and the Penetration Filter was turned "off". Other filters typically used in the ON position were sector tracking and interference with occasionally aeration and slope filters turned "on" in rough weather. No automatic cleaning was done to the data.

In terms of processing, the raw *.all data were converted to MB-Systems format *.mb59 files using a script and then processed in the MB System software where ping editing was done and files saved as trackline swath grids. The following steps were followed in processing the multibeam data:

1) Go to the "ship data" drive and copy all newly written .all files into the "allFiles" folder
2) Start Cygwin, type "startx" command to begin MB Systems
3) Navigate to "allFiles" and run the "./all2mb.txt" command to parse the various ".mb59" file types
4) While this is being done, create a new folder for the next 4 sets of files to be processed (i.e. MBJQ0654_0657)

5) Once the "./all2mb.txt" command has completed, Cut and Paste the next 4 sets of files into the folder just created, as well as copying in the "postedit_gridmaker.txt" file and navigate to this folder in Mb Systems
6) Apply the Limit Excessive Angle Filter via MBClean to each of the ".mb59" files
    a. (i.e. mbclean -I 0654_20111127_114048_TGT.mb59 –C40/2)
7) Once complete, begin manual editing via the "mbedit" command, erasing/restoring as necessary
8) Once all files are completed and saved, quit mbedit and run the "./postedit_gridmaker.txt" command in order to create a .grd file
9) Rename the .grd file, copy the .grd file into "MB.grd Files" folder on cruiseshare drive and import the .grd file into Fledermaus
10) If necessary, go back into mbedit in order to correct any parts of file not edited correctly (such as minor "spikes"/"walls")
11) Adjust color scale if necessary and save as screenshot with color legend
12) Repeat steps 4-12.

Knudsen 3260 Chirp Sub-Bottom Profiler

Shallow sub-bottom acoustic profiling was carried out using Knudsen Chirp 3260 3.5 kHz onboard the vessel (system parameters can be found in Table 3). The ship also has a Knudsen 320B/R multi frequency echosounder system (2.5-250 kHz) that can be used to obtain water depth directly below the vessel in 12 kHz mode. During this cruise we employed the Knudsen-3260 in 3.5-kHz-mode, allowing the acoustic signal to penetrate below the seafloor. The quality and the maximum penetration depth vary depending on the bottom characteristics. In general, sub-bottom profiler provided sediment structure of 150-200 mbsf. Sound speed is entered as a fixed value and we used 1490 m/s for the cruise. The output display monitor only had a fixed scan of 1 second available, which required changing the depth window being displayed when bathymetry varied substantially. Data was output and saved in various formats including SEGY and XTF formats as well as the proprietary Knudsen KEB binary format and an additional KEA (ascii format). During Sentry dives the Chirp was switched off and the system was used to listen in "pinger" mode. The system was set to listen to 11 kHz although all relevant long-baseline frequencies are detected (8,12,14.5 kHz). During deployments, the pinger record would show Sentry's descent and when Sentry dropped its weight to start its survey as well as when it released its ascent weights and started back to the surface. Sentry transponder signals were on a 20 sec period. If the Sentry sub-bottom sonar was turned on, it would also show up as a record with an outgoing ping and bottom return twice on the display, as it was running at 2 Hz.

Typical settings used for the chirp underway sonar surveys are summarized in the table below. The power level, pulse length, fixed gain, and time varying gain (TVG) were sometimes changed for better clarity of features on the record sheet.

Preliminary interpretation of bathymetry and chirp-sonar data can be found in Appendix 2.

Gravity

Marine gravity was obtained with a BGM-3 gravimeter [Bell and Watts, 1986] (Fig. 11). The Thompson's gravimeter, serial number S210 was installed on the Thompson in May 2011 and prior to the cruise was running well. In-port tests were conducted in Honolulu along with a gravity tie to the absolute gravity station at the University of Hawaii pier. At the end of the cruise, a gravity tie was performed at Victor pier at the U.S. Navy base in Guam. The absence of a land gravity station at Victor pier required a tie to an existing station at Tango Pier.

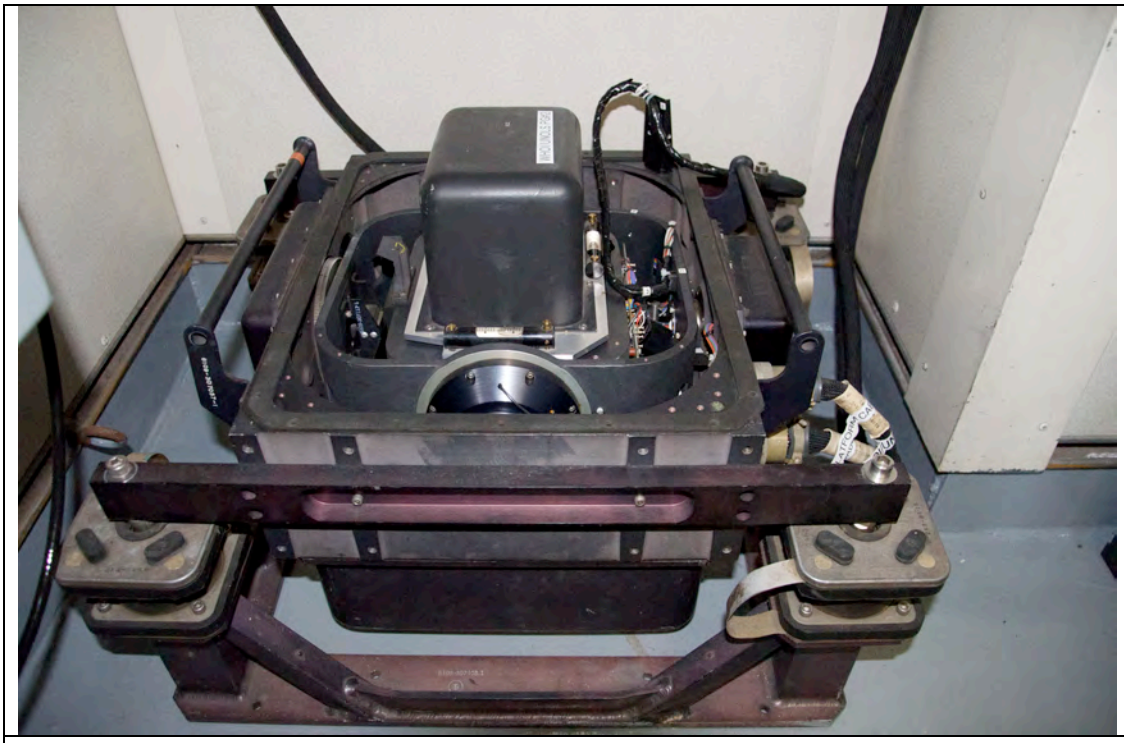

Figure 11. BGM-3 Marine gravimeter

The gravimeter worked well throughout the cruise and no hardware problems were encountered. No sensor errors were detected and platform errors (which occasionally occur because of increased sea state or ship turns) occurred less than 0.1% of the time.

Data was logged with software developed at WHOI that provided co-registered raw gravity counts, ship's navigation (latitude, longitude, heading, speed over ground, and course over ground), and seafloor depth. This data is logged at the native 1Hz rate of the BGM-3 gravimeter in a raw gravity string (RGS) file. The file closes out every 24 hours and provides all the data necessary to reduce the gravity.

Prior to processing the gravity data, we culled obvious errors from the RGS files. For the most part, those errors included where the ship's GPS was clearly erroneous (e.g., latitudes <10 or >30 or longitudes <-180 or >180) or where errors were flagged by the gravimeter. We removed lines where the ship's echosounder recorded depths of <5 meters, which are unrealistic, and lines where the echosounder was turned off (the frequency of the sounder is similar to that of AUV-Sentry's communications systems, so the sounder was turned off during Sentry dives). Some of these data could be recovered if an independent measurement of depth is obtained. Finally, we removed lines recorded between 4:20:56 and 4:21:15 on 11/11/11, when the ship crossed the meridian. When we entered the Easter Hemisphere, the GPS took 21 seconds to level out with new longitudes.

The observed (raw) gravity values measured on the ship include contributions stemming from the acceleration of the ship in various directions. The most obvious of these include accelerations caused by the heave of the ship. To mitigate these effects, we applied a six-minute, one standard-deviation Gaussian filter to the raw gravity values, which effectively cancels out the high-frequency movements of the ship. The gravity values also include accelerations due to the ship traveling to the east or west that reduces or increases the gravity, respectively. These accelerations can be removed using the Eötvös correction:

$$E_c(mGal) = 7.503S\ \sin H\ \cos f + 0.004154S^2$$

where S is the ship speed (knots), H is the heading, and f is the latitude. The correction values were also smoothed by a six-minute, one standard-deviation Gaussian filter to mitigate the effects of changes in the ship's heading and speed data. (We tried smoothing the input values rather than the Eötvös corrections themselves, but the difference was negligible, i.e., <0.05 mGals.)

The remaining smoothed include gravity variations due to the attraction of the reference ellipsoid, and the elevation of the gravimeter above the geoid (free-air), the topography of the sea floor, and the effects of density and isostatic variations in the upper mantle and crust (anomalies). We used the reference ellipsoid given by the Geodetic Reference System Formula (Woollard, 1979), where the value of g at latitude f is given by:

$$g_f(mGal) = 978031.846\left(1 + 0.005278895\ \sin^2 f + 0.000023462\ \sin^4 f\right)$$

Because we are above sea level, the free-air correction should be added to the observed gravity. The gravimeter on the Thompson is on the deck closest to the ship's water line (~1 meter above sea level), so our height (h, in meters) above the geoid is small:

$$FAC(mGal) = 0.08633h$$

The topography of the sea floor is measured by the ship's echosounder. We applied a two-minute, one standard-deviation Gaussian filter to the depth measurements in order to

mitigate some high-frequency noise present in the data. The smoothed depths were used to calculate the Simple Bouguer Correction:

$$BC(mGal) = 2\pi \mathrm{G}\left(r_b - r_w\right) d_{filt} \ *10^5$$

where *G* is the Universal Gravitational Constant (6.67 ´ 10^{-11} m^3 kg^{-1} s^{-2}), r_b is the density of the seafloor topography (2670 kg m^{-3}), r_w is the density of seawater (1000 kg m^{-3}), and d is the water depth in meters.

With these numbers, we calculated the free-air gravity anomaly and the Bouguer anomalies using the filtered gravity, filtered Eötvös corrections, free air corrections, and simple Bouguer Corrections:

$$Dg_{FAA}(mGal) = \left(g_{filt} + E_{c,filt} + FAC\right) - g_f$$

$$Dg_B(mGal) = \left(g_{filt} + E_{c,filt} + FAC + BC\right) - g_f$$

The culled and processed data is recorded in CSV files (RGSfilename.cull.proc) with columns that include the following: calendar date, time, unix time, raw gravity (mGal), filtered gravity (mGal), ship speed (knots), ship heading (decimal degrees), latitude (decimal degrees), longitude (decimal degrees), Eötvös correction (mGal), filtered Eötvös correction (mGal), height of the gravimeter above the geoid (m), free air correction (mGal), echosounder depth (m), filtered echosounder depth (m), Bouguer correction (mGal), Geodetic Reference System Formula result (mGal), calculated free-air anomaly (mGal), calculated Bouguer gravity anomaly (mGal).

7. Seismic Systems

Reflection Seismics

The seismic component of the Jurassic Crust Magnetic Survey was designed to distinguish between "unmodified" Jurassic crust and crust that has been overprinted by Cretaceous volcanism and, where identified, to characterize the Cretaceous igneous additions to the crust (e.g. sills, dikes, flows, volcaniclastics, seamounts). Igneous basement/top of massive Cretaceous volcanic flows are visible in our reflection profiles. In some areas, the data image discontinuous, low frequency reflections that may represent structure within the oceanic crust. Using these data, combined with the refraction data from sonobuoys, we will attempt to distinguish Jurassic oceanic crust from younger, intruded Cretaceous volcanics and characterize the tectonic structure and sedimentation history of the Jurassic-age Pacific Plate.

Instrumentation

We used the Scripps Institution of Oceanography high-resolution multi-channel seismic (MCS) system to collect seismic reflection data during the cruise. This system consists of an 870-m-long, 48-channel Geometrics GeoEel streamer and a 2-GI-gun cluster (Fig. 12,

Appendix 3). We shot on distance meaning that our shot spacing of 25 meters was tied to ship speed and navigation. During seismic operations, we traveled an average speed of 4 knots. The decision to shoot on distance rather than time was tied into the collection of seismic refraction data using sonobuoys deployed approximately every 16 kilometers along the survey line.

In total we have over 800 kilometers of seismic profiles. Lines 1, 2, 7, 8, 9, and 10 trend NE-SW following the magnetic survey line. The others, Lines 3-6, make up the additional seismic surveys (Fig. 13). Onboard the Thompson, the Scripps team created seg-y and navigation files using SioSeis and Jinchang (Sam) Zhang processed the MSC data through to time migration using ProMAX (Appendix 4).

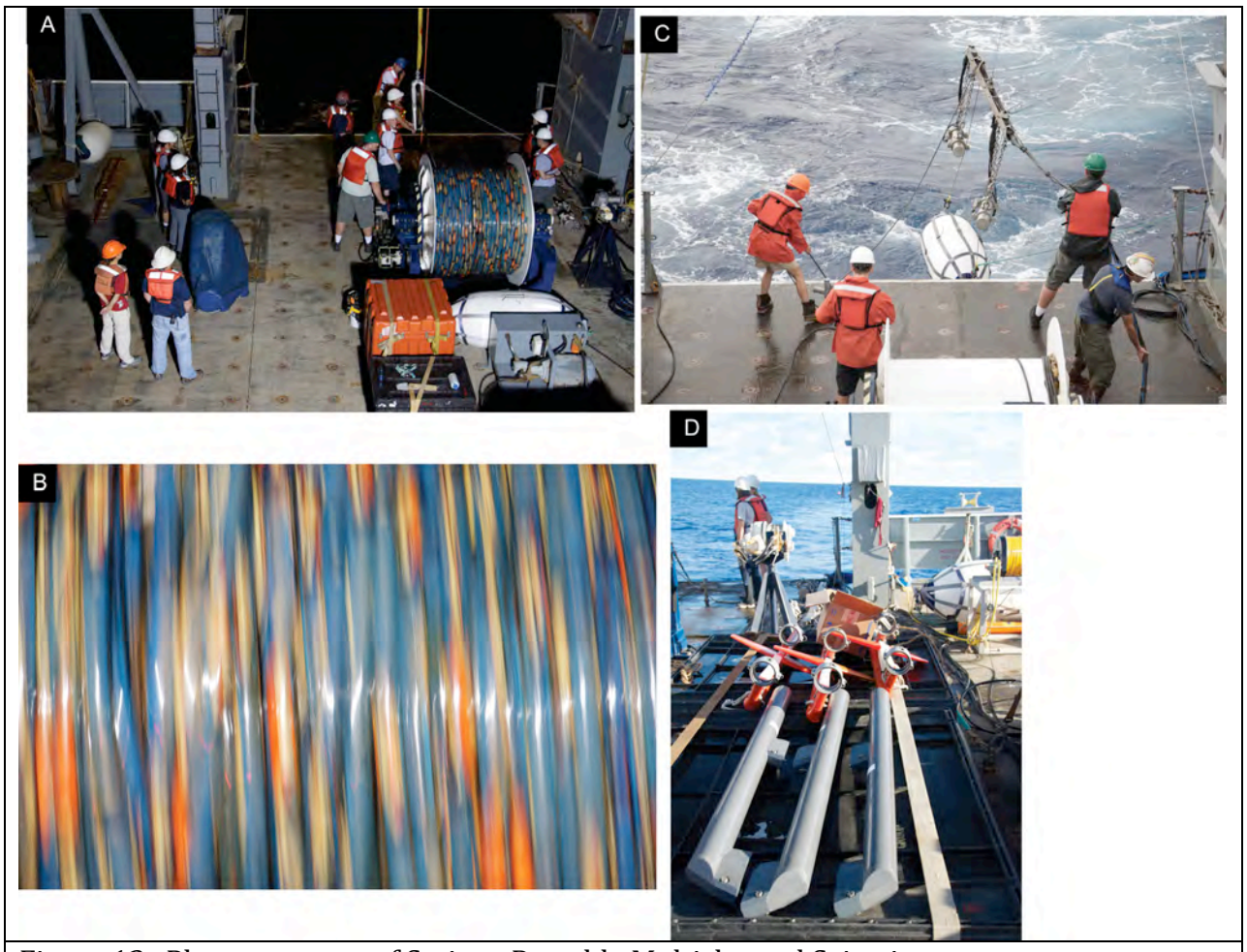

Figure 13. Photo montage of Scripps Portable Multichannel Seismic system

Survey Plan

Initially, seismic operations were conducted during the 16-hour AUV-Sentry battery recharge cycles. Gear deployment and recovery time took approximately 3 hours during

each operation. With added travel time, we had less than nine hours for data collection. Changes in the cruise plan because of weather and technical difficulties with Sentry resulted in continuous shooting of seismic data for periods of 30 hours up to over 3.5 days. Because weather early on in the cruise was too rough to launch Sentry or TowCam, we had time to add two extra seismic surveys, which will strengthen our overall interpretations of this area. We did not deploy sonobuoys during these supplemental surveys. In addition to our long line running NE-SW across magnetic lineations, perpendicular to spreading, we completed two surveys orthogonal to our main line. The first consists of relatively short lines making a box around our initial survey in a region of interest. The second additional survey line trends NW-SE for ~54 km, parallel to the direction of spreading. This survey was designed to image the plate in the region of a possible fracture zone hypothesized from the interpretation of satellite gravity models (http://www.soest.hawaii.edu/PT/GSFML/). These extra seismic lines provide some 3-dimensional control on our interpretations. We will also be able to investigate changes in the Jurassic Pacific Plate structure and sedimentation both parallel and perpendicular to spreading direction.

For first of these surveys (lines 3-5, Fig. 13) we shot on time instead of distance because of problems with the PosMV GPS navigation system. Erroneous GPS points occasionally caused the guns to misfire because the 25 meter shot interval was exceeded in less than 12 seconds. Switching to time, shots were fired every 12.5 seconds to maintain a shot interval of approximately 25 meters, depending on ship speed. During these surveys we logged ship speed over ground (SOG) every 15-30 minutes. We maintained a slightly shower speed during this survey (~3.5-3.8 knots) because the high sea state was causing noise to wipe out most of the far channels (43-48) on the streamer. The tail buoy bounced with the high wind and waves and the birds struggled to keep the streamer at a constant depth near four meters. Lines 3 and 4 appeared especially noisy in the real-time near trace gather, and although much of this noise was removed during stacking, the data from this part of the survey overall are lower quality than on the other seismic lines.

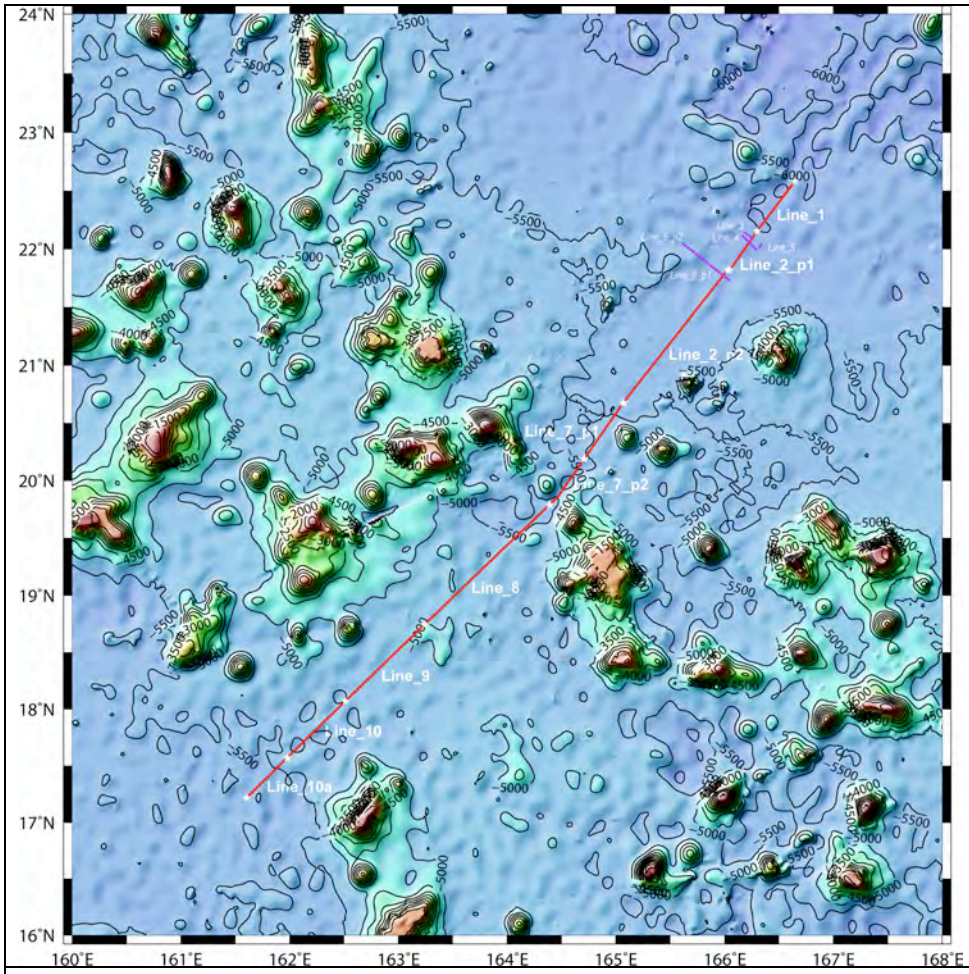

Figure 13. Map showing the TN272 seismic tracklines

Although we continued to have problems with the navigation tied to the seismic system we returned to shooting on distance for seismic line 6 and for the remainder of the seismic survey. Problems with the navigation system caused gaps in data on MCS lines 6 and 10. For line 6, the ship drifted too far off of the programmed seismic line and data were not recorded for several minutes. On line 10 the guns stopped shooting for ~5 minutes. During the time that we shot seismic continuously for more than 3.5 days, we broke up our survey into 4 lines, to make data storage and processing more manageable. These line switches took less than two minutes, representing less than 12 shots, and did not result in any data gaps.

Preliminary Interpretations

Figure 14 shows all of the MSC lines plotted as a continuous survey. Our seismic survey was conducted along a corridor that minimizes the influence of Cretaceous volcanism, avoiding known seamounts; however, we encountered previously unmapped seamounts as well as igneous flows and sills. The data image thick sediment packages, likely including chert, turbidites and marine snow, igneous basement and, where present, sills intruded into sediment. The sills appear as strong, high frequency reflections that obscure any deeper

structure. Some of the sills interpreted from the MSC reflection data were visible in preliminary interpretations of sonobuoy data (e.g. L2). In some regions, low-frequency, discontinuous horizons are visible beneath basement, especially when a bandpass filter of 5-8-60-70 was applied to the data. This filter is only useful for imaging the deeper structure and completely wipes out the higher frequency sediment layers and the seafloor horizon.

Lines 1 and 2 trend NE-SW, covering relatively flat seafloor that shoals to the south. The northern part of our seismic survey (Lines 1-5) image a thick (~378 ms) sediment package. This package includes a uniform layer of nearly transparent sediments draping the lower structures (64 ms thick), and likely represents abyssal clays deposited as marine snow. Below this are strong, uniform reflections for ~87 ms. The CHIRP sonar system on board could not image below these strong reflections. It is likely that this section of the sediment package includes the chert layer described by Abrams et al. (1993), and may also represent turbidites. Below this high frequency, banded sequence is a thick layer of alternating transparent and banded horizons down to the "basement" horizon (~227 ms). Most of the potential sills we have identified are located in this lower sediment package. The sediments are pulled up by what appear to be small volcanic intrusions, which cause a localized high on the seafloor. The data image a possible basement horizon near depths of 8350-8150 ms TWTT. This horizon, at the base of the sedimentary section, is prominent and easy to identify except when obscured by high frequency, strong reflections within the sediment layers, likely sills. It some areas the basement appears to be on the second portion of line 2, the basement horizon shallows gradually from 8300-7900 ms and there is overall thinning of the sediment package.

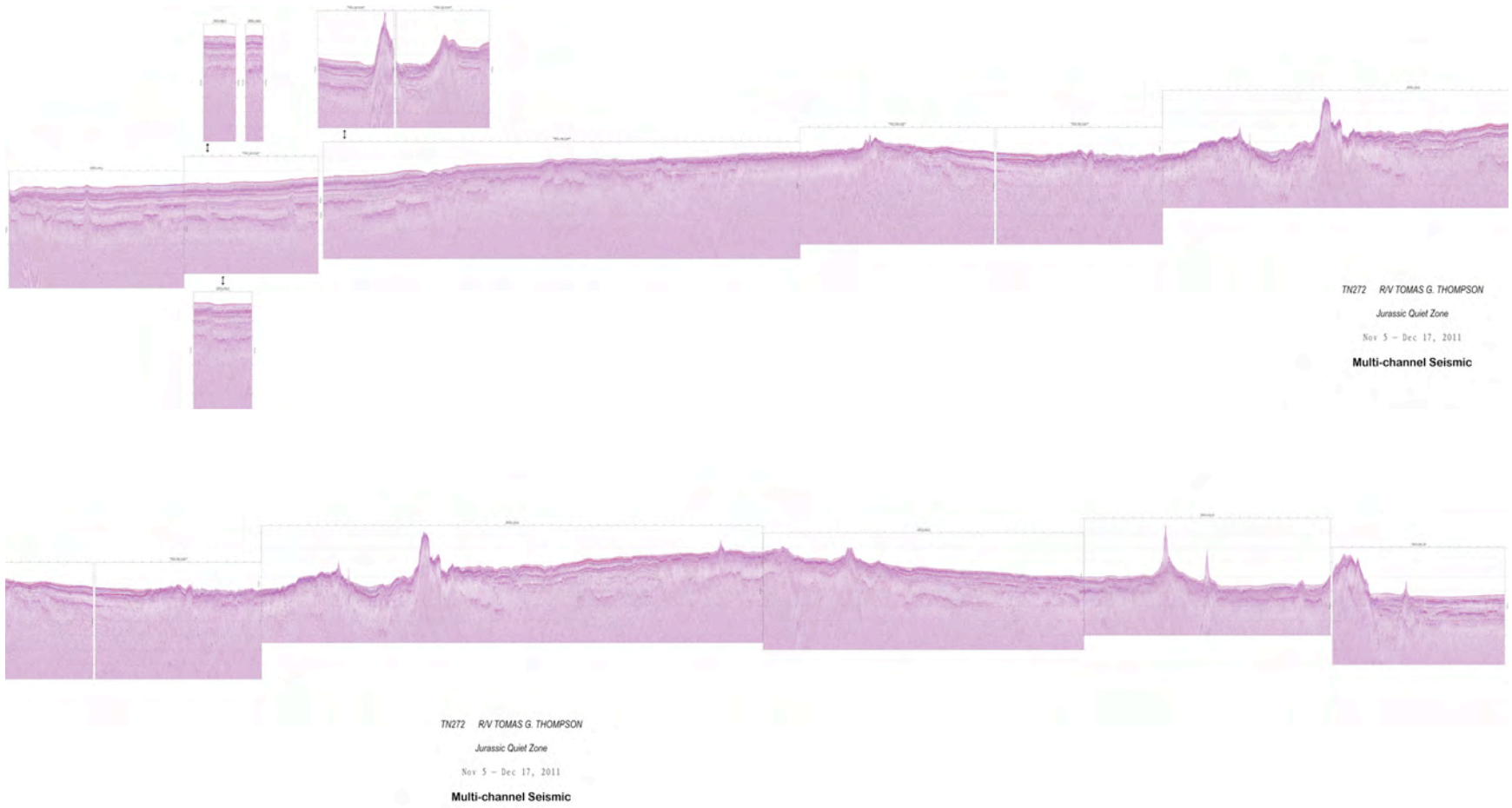

Figure 14. Summary MCS profile

Refraction Seismics

During seismic operations on TN272, 50 sonobuoys were deployed at 16 km intervals and their radio signal recorded to provide data with which to investigate the possible presence of abnormal Jurassic crustal structure produced by volcanism during the Cretaceous.

Equipment

Fifty sonobuoys purchased from Ultra Electronics (Dartmouth, Nova Scotia) were stored in their wood shipping container at the aft end of the staging bay on the main deck. The receivers were modified military-type DIFAR AN/SSQ-53D(3) omnisensitivity sonobuoys manufactured in November 2010 (Ultra Electronics PO E112980). The manufacturer rates the operating frequency band to 5-2,400 Hz. Figure 15 shows that the frequency response of the 'modified' 53D sonobuoys provided by the manufacturer peaks at 40-50 Hz with 10 db down points at 9 Hz and 310 Hz.

Radio signals were received on the ship with a Sinclair Model SY2062-SF2SNM(C) antenna. This model is a dual stacked, 12 dBd, center mount, 152-159 MHz YAGI antenna. The antenna was mounted on 1.5 in diameter pipe at 10' height above the starboard end of the flying bridge at about 9 m off the ship's centerline along frame 57. The flying bridge is 54 feet (16.5 m) above sea level, so the antenna is mounted at about 64 feet (19.5 m) above sea level. A Yaesu Model G-450A rotation motor was installed as part of the antenna mount and cabled to a controller box in the computer lab, so the antenna could be rotated if we suspected strong currents carried the sonobuoys off the ship track. Figure 16 includes pictures of the antenna installation.

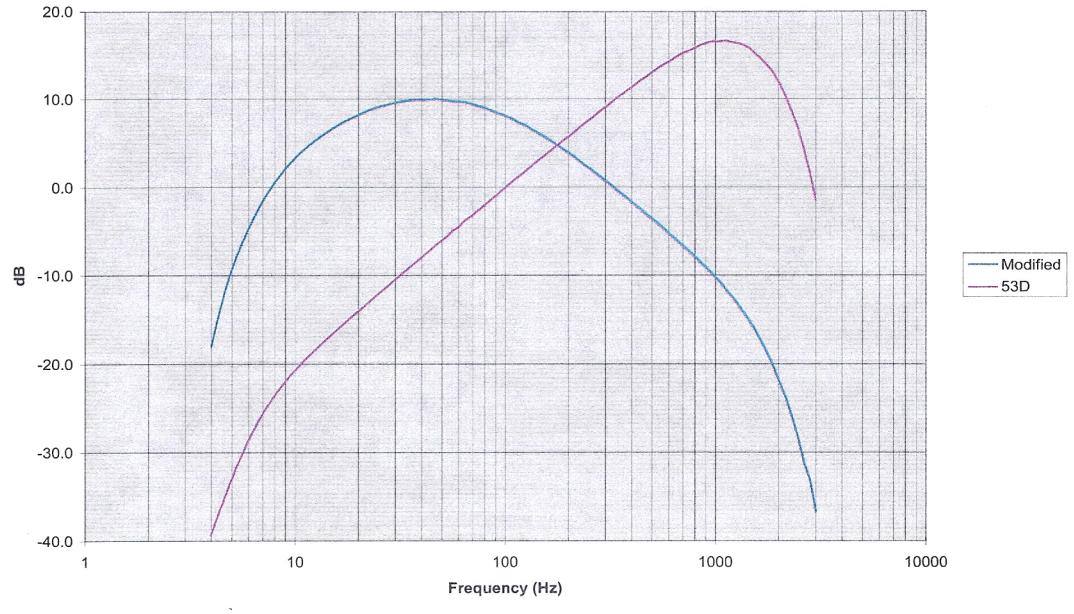

Figure 15. Frequency response of modified military-type DIFAR AN/SSQ-53D sonobuoy.

The antenna signal was cabled to the computer lab and into a WinRadio Model WR-G39WSBe receiver, which could be controlled by WinRadio software on a Dell PC. The de-modulated signal was run in series through two Krohn-Hite Model 3700 analog filters each set to pass 1-150 Hz with zero gain. The filtered output was split so the signal could be recorded as an auxiliary channel by the multi-channel seismic (MCS) system and as channel one by a Ref Tek RT130. The airgun trigger signal from the MCS fire-control system was recorded as channel two of the Ref Tek 130. The RT130 digitized both signals at 500 Hz and recorded them in Ref Tek compressed format. A gain of 32 (high) was applied to the sonobuoy signal; a gain of one (low) was applied to the gun trigger. We switched from Ref Tek 130 S/N 991F to S/N 9873 between seismic lines 1 and 2. The MCS recorded seismograms at 1000 Hz with a pre-amp gain of 18 db for streamer channels and 0 db gain for the auxiliary channels (including the sonobuoy channel). No frequency filtering was done by the MCS system prior to digitizing for either the streamer or the sonobuoy channels.

GPS time and ship location were continuously recorded by the Ref Tek 130 using a feed from a Garmin 16-HVS GPS receiver (labeled "Ref Tek RT 130 GPS-02 S/N 6509") mounted on the 02 deck about one meter to port of the centerline of the ship on ship frame number 91 at an elevation of 45 feet (13.7 m) above sea level. Figure 16 includes pictures of the RefTek GPS installation. Test of the integrity of the system were made while at the dock and while underway prior to operations using a test sonobuoy disabled for us by the manufacturer.

Figure 16. Photo montage of sonobuoy antenna installation.

Processing

After the airguns were turned off at the end of each seismic line, the Ref Tek 130 was allowed to record data for an additional 10-15 minutes before terminating acquisition. Disk utilization was noted and the Ref Tek was left powered for an additional 0.5-1 hr before the power was turned off and the current compact flash card removed. Software provided by Passcal (Nero) was used to copy the data off the card onto a MacBook using a Kingston FCR-HS219/1 card reader. The compressed data in zip files created by Nero were reformatted to MiniSeed using Passcal software (rt2ms). Another Passcal program (pql) was used to inspect the time series and compute spectra. ProMAX seismic processing package (Landmark) was used to make a record section from the auxiliary channel of the segd file recorded by the MCS system. We plotted the sections with GMT, and a screen capture was used to print the sections. Figure 17 shows a sample record section of SB#3. Appendix 5 contains a copy of all plots. All data files were archived to a 500 Gb Lacie drive.

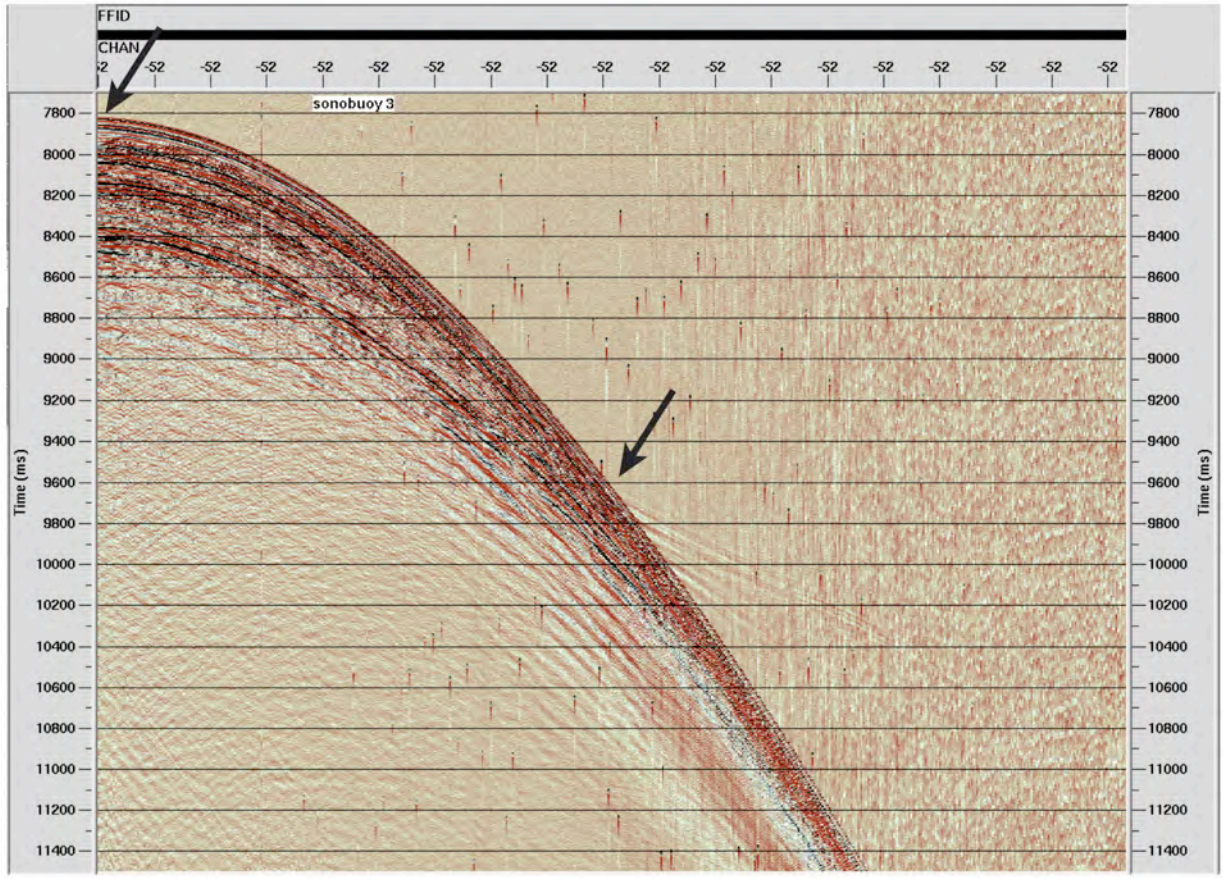

Figure 17. Example of sonobuoy profile.

XBT Sound Speed Profiles

Knowledge of vertical sound speed variations in water will be useful in ray-trace modeling of sonobuoy seismograms. Depth profiles of sound speed were obtained from both XBT temperatures and from temperature, salinity, and pressure measured by a SeaBird SBE 49

CTD mounted on Sentry during dives along the survey line. Table 4 contains details of the XBTs, and Figure 18 shows a map of the XBT stations. The acquisition software computed sound speed assuming a constant salinity (given in Table 4). Sound speed variations with depth (Fig. 19) follow the trend from gridded historic data (S. Levitus, Climatological atlas of the world ocean, NOAA Prof. Paper 13, 173 pp., 1982, obtained using MBSystem) except where they systematically exceed the historic average by ~5 m/s in a prominent well-mixed layer in the upper 100 m.

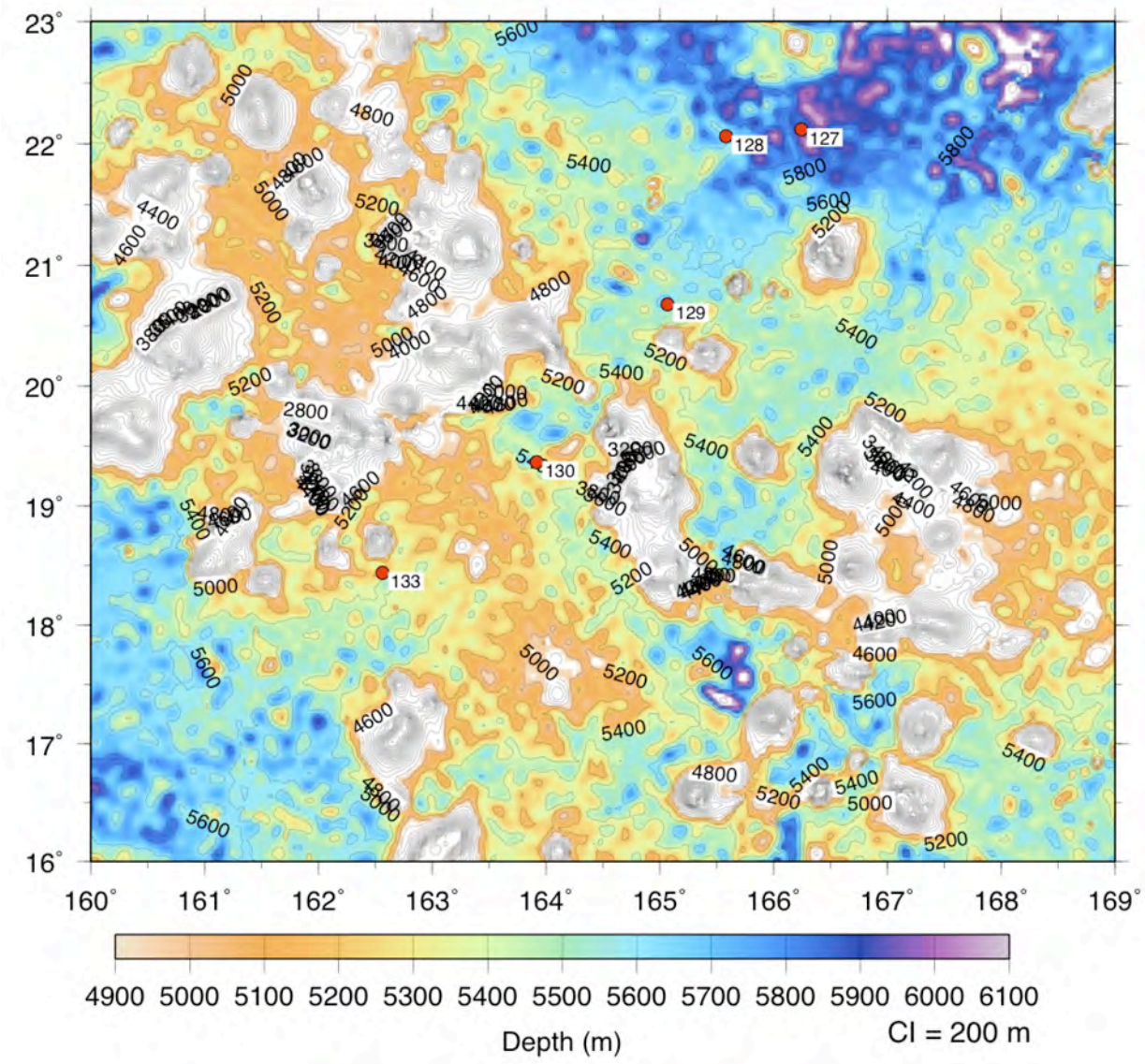

Figure 18. XBT sound profile launch locations.

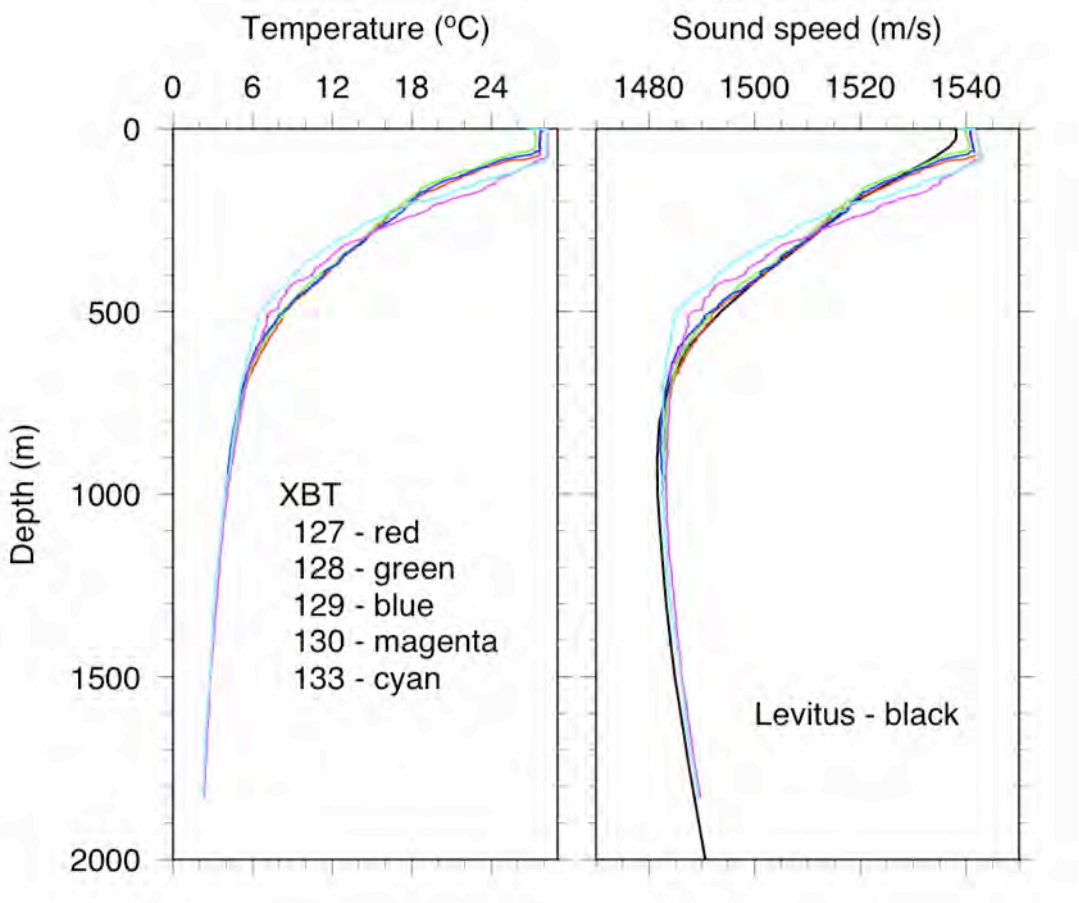

Figure 19. Sound speed profile

To compute depth and sound speed for the SBE 49 data from Sentry, we ran Matlab scripts written by P. Morgan (CSIRO) using algorithms from Fofonoff and Millard (Algorithms for computation of fundamental properties of seawater, UNESCO Tech. Paper in Marine Science 44, 53 pp., 1983). Initial results showed that salinity more often appeared to be reasonable during Sentry's ascent than during her descent - probably due to slow flushing of tubing leading to the salinity sensor at the start of the dives and, perhaps, warming of the sensor by the thermal mass of Sentry. Table 5 contains dive locations, and Figure 20 shows locations of the recovery positions of Sentry, which are a good approximation for the location of the ascent CTD profiles. Dives 130-131 are shallow water test dives. Figure 21 shows profiles of temperature, salinity, and sound speed. Conductivity values during dive 130 remain near 0.02-0.03 throughout the dive indicating that the sensor failed; sound speed values for this dive are unreasonably low. The salinity profiles for dives 128 and 134 are anomalous also indicating problems with the sensor. As a result, values of sound speed for dives 128 and 134 are untrustworthy. With two exceptions, sound speed profiles from Sentry follow Levitus. (1) In the upper limb of the sound speed channel between 250 and 750 m depth, sound speed from Sentry is up to 10 m/s slower than Levitus. (2) Sound speed is 5-10 m/s faster than Levitus in a well-mixed layer in the upper 60 m. There is some indication that the thickness and sound speed of the well-mixed layer increase during

the course of the survey, perhaps indicating turbulent mixing caused by 20-30 kt winds encountered and solar warming of the sea surface.

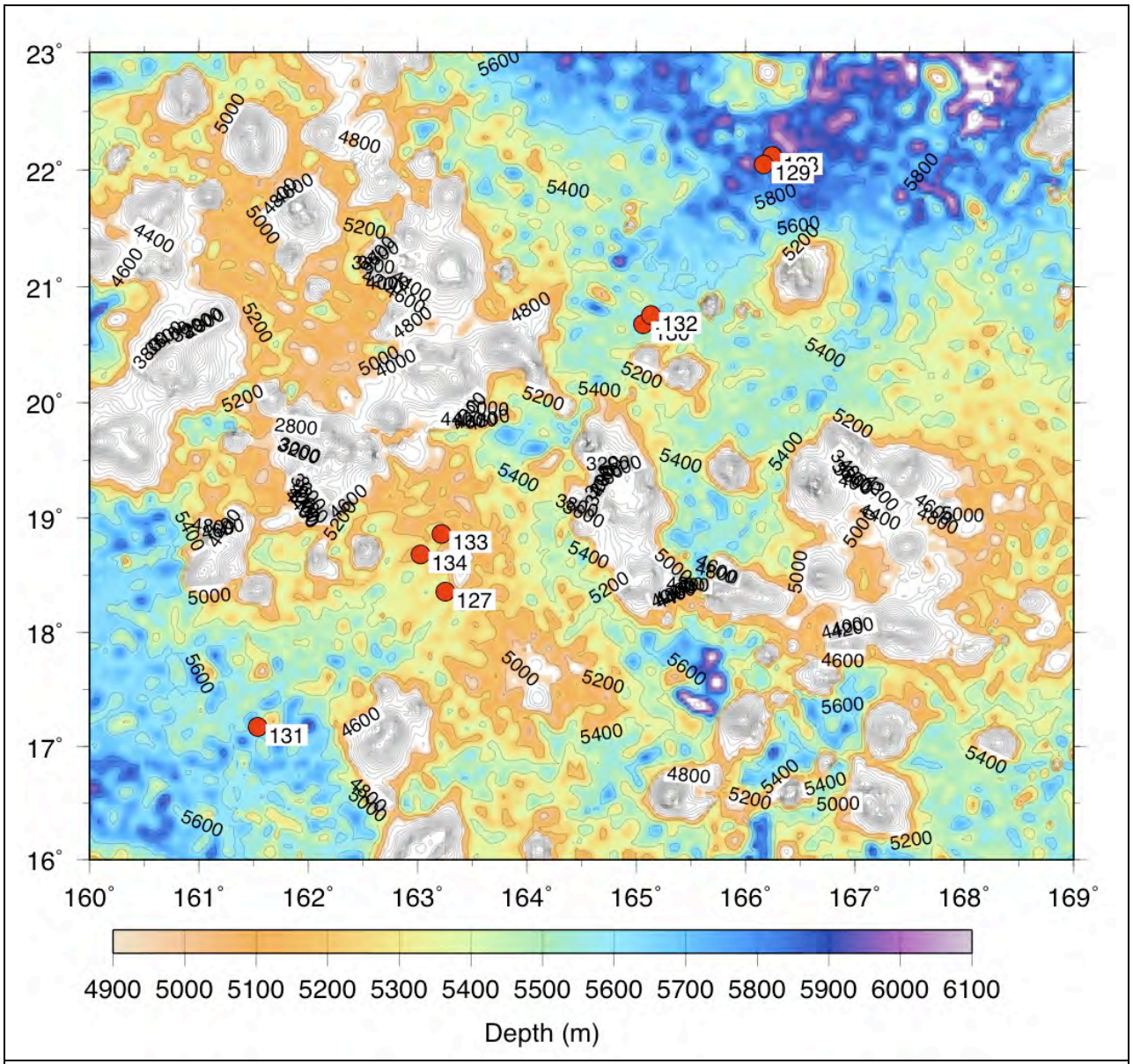

Figure 20. Recovery positions for Sentry

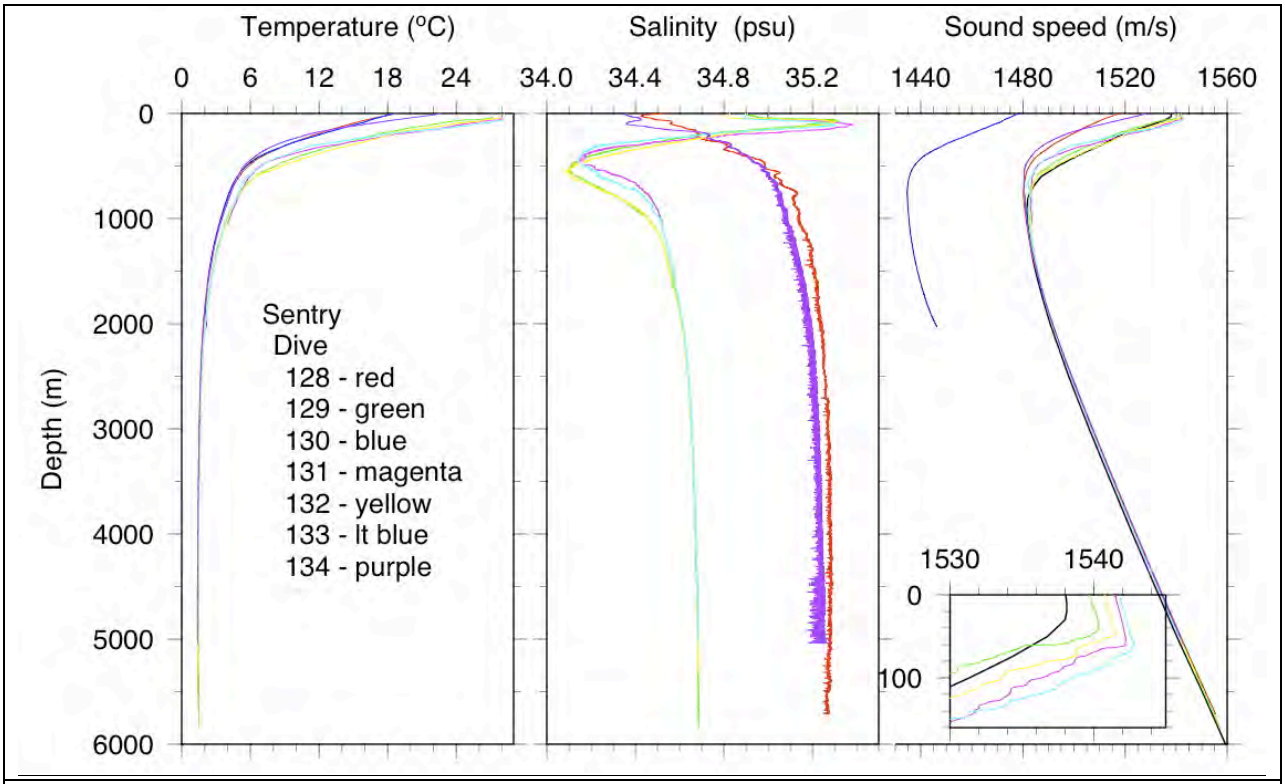

Figure 21. Sentry temperature and salinity profiles from dives.

Sonobuoy Geometry

Knowing the range from each airgun shot to the active sonobuoy receiver is essential to interpret the sonobuoy seismograms. Range is computed from the location of each shot and the location of the sonobuoy at launch assuming that the sonobuoy does not drift. For this experiment, the location of each airgun shot can determined using the offset of the airgun array from the point on the ship to which the P-code GPS fixes are referenced. Appendix 4 contains figures showing the offsets from the airguns to the Inertial Motion Unit (IMU). The IMU is located along the starboard wall of the engineers' office on the platform deck (ship frame 53, 1.5 m port of the centerline). The NEMA strings recorded in the seismic segd headers and provided to Swift in ascii files for each line ("TN272.*.Nav.txt") contain P-code GPS locations from the "PosMV" navigation system after being shifted to the location of the IMU. The ship locations recorded in the shipboard "DAS" data logging files and recorded by the sonobuoy watchstanders at the time of launch come from the "C-Nav" P-code GPS system. Figure 22 shows the schematic locations of the key spots on the ship relevant to sonobuoy operations, and Table 6 provides the offsets to the IMU. It is important to note that the watchstanders recorded the time that the sonobuoy hit the water surface, so a further correction must be applied. Sonobuoys launched from the main deck (SB# 1-3) landed about 1.5 sec after being thrown; they hit the water about 3 m aft of their launch position (assuming a ship speed of 4 knts – 2 m/sec) and 2-3 m outboard. Sonobuoys launched from the 02 deck (SB# 4-5 and 7-50) landed about 3 sec after being thrown; they hit the water about 6 m aft of their launch position and

3-4 m outboard. The one sonobuoy thrown from the bridge deck (SB# 6) landed about 4 sec after being thrown; it hit about 8 m aft of its launch position and 3-4 m outboard.

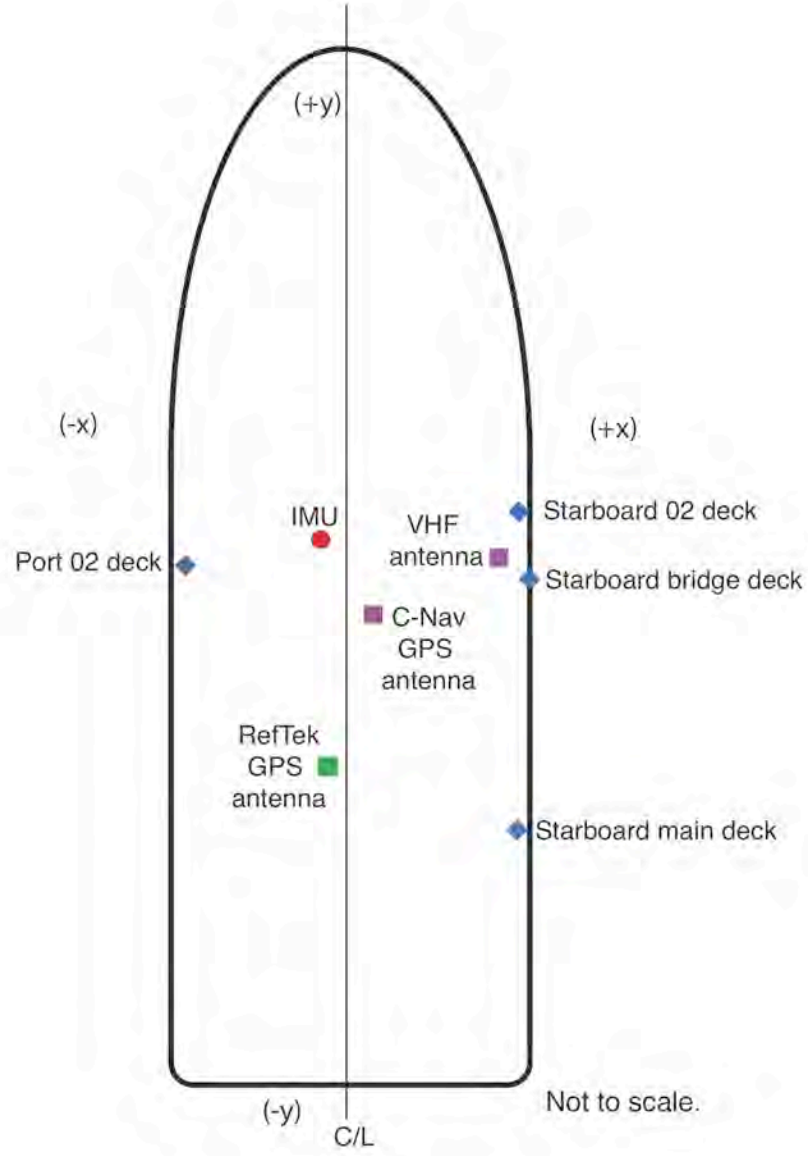

Figure 22. Antenna locations

Launch Protocol

Prior to start of seismic operations, power was turned on to the Krohn-Hite filters, the radio receiver, Ref Tek 130, and PC. The sonobuoy channel was selected using the Win Radio software on the PC, and acquisition was started on the Ref Tek 130. Enough sonobuoys for the up-coming seismic line were removed from the shipping container and stored on a table top in the main lab. Operations typically required three people: one to carry and throw the sonobuoy and a radio operator to call back to the lab at the instant the buoy hit the water, and a data logger positioned by a ship data screen in the computer lab.

Sonobuoys were removed from their plastic shipping tubes, and the wind flap and parachute netting were disconnected. The radio channel, buoy life, and hydrophone depth were programmed. The WinRadio display usually showed higher background noise on channels above channel 48 (>142.000 Mhz), so we used only channels 32-48 (136.000-142.000 Mhz). The scuttle time for the buoys was always set to 8 hrs (choices – 0.5, 1, 2, 4, 8 hrs). The hydrophone depth could be set to d1 (100' – 30.5 m), d2 (200' – 61.0 m), d3 (400' – 122 m), or d4 (1000' – 305 m). Buoys were thrown over the starboard rail on the main deck, the starboard 02 deck, the bridge deck (once), or the port 02 deck (Fig. 22, Table 6). The float usually emerged within 10-15 sec and was observed to drift aft to the outboard of the streamer. Buoys were launched at 16 km intervals starting at the beginning of each seismic line.

Seismic Operations

Table 7 provides details of the sonobuoy deployments; Table 8 gives the MCS line number and shot number at the launch and termination of each buoy. Figure 23 shows the locations of launch positions on a map of satellite-derived bathymetry. Lines 1-2 were shot at a ship's heading of ~218°. The azimuth of the survey line changed to ~225° between sonobuoys 24 and 25. For buoys that returned a signal, Figure 24 shows the decay with time in the amplitude of the Win Radio signal on the transmission channel. Although very short spikes of high amplitude appear during every shot, we recorded the background amplitude. Thus, Figure 24 probably represents the strength of the sonobuoy's carrier signal. Most buoys follow a pattern of amplitude decay with time that resembles a $1/r^2$ pattern. Sonobuoys 5 and 24 had unusually weak signals throughout the ~ 2 hours that we monitored them.

During seismic line 2, which was exceptionally long, the sleep function on the PC would activate and hang up the computer. When this occurred, we shut down the PC using the power switch before re-booting the PC and the Win Radio software. Using the PDA and the monitoring functions provided with the RT 130, we found that the receiver continued to send seismic signal to the RT 130. So, the Win Radio software is not required to operate the Win Radio receiver itself. We disabled the sleep function before later seismic operations.

Line 1

All four buoys were launched with the hydrophone depth set to D1 (30.5 m). ADCP surface currents were consistently 1-2 knots to the SW parallel to the shooting line; winds were generally 8-12 knots to the west and to the west-northwest. The sonobuoy signal monitored by the RT130 for SB 1 appeared to have exceptionally better signal-to-noise character than for SBs 2-4. However, the MCS channel gather shows that only the first 5% of the shots for SB 1 were recorded on the MCS auxiliary channel. In retrospect, it is likely that inexperience lead us to interpret a persistent random noise chirp as a clean airgun signal. If this interpretation is true, then Sonobuoy 1 must be added to the list of failed buoys (Table 7). Figures 25 and 26 show a sample time series and a spectrum of the noise chirp recorded after the airguns had been turned off at the end of Line 1. The signal is predominantly a 1 Hz oscillation that decays with time. It is present throughout the

sonobuoy data. The amplitude of the chirp does not appear to vary during the survey indicating that the chirp is not transmitted from the buoys whose signal decays with time (Figure 24). The noise source must be on the ship).

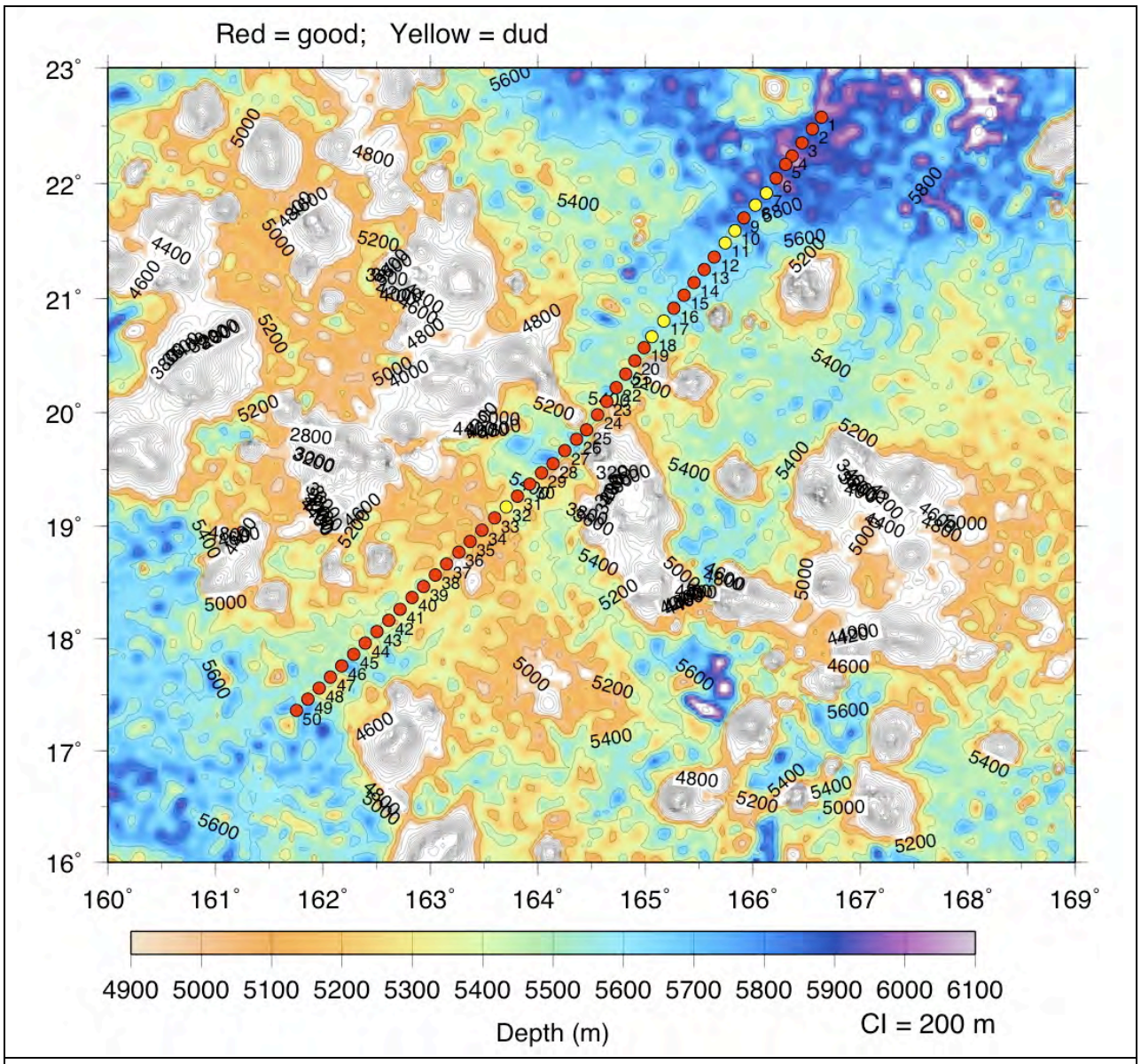

Figure 23. Sonobuoy launch positions

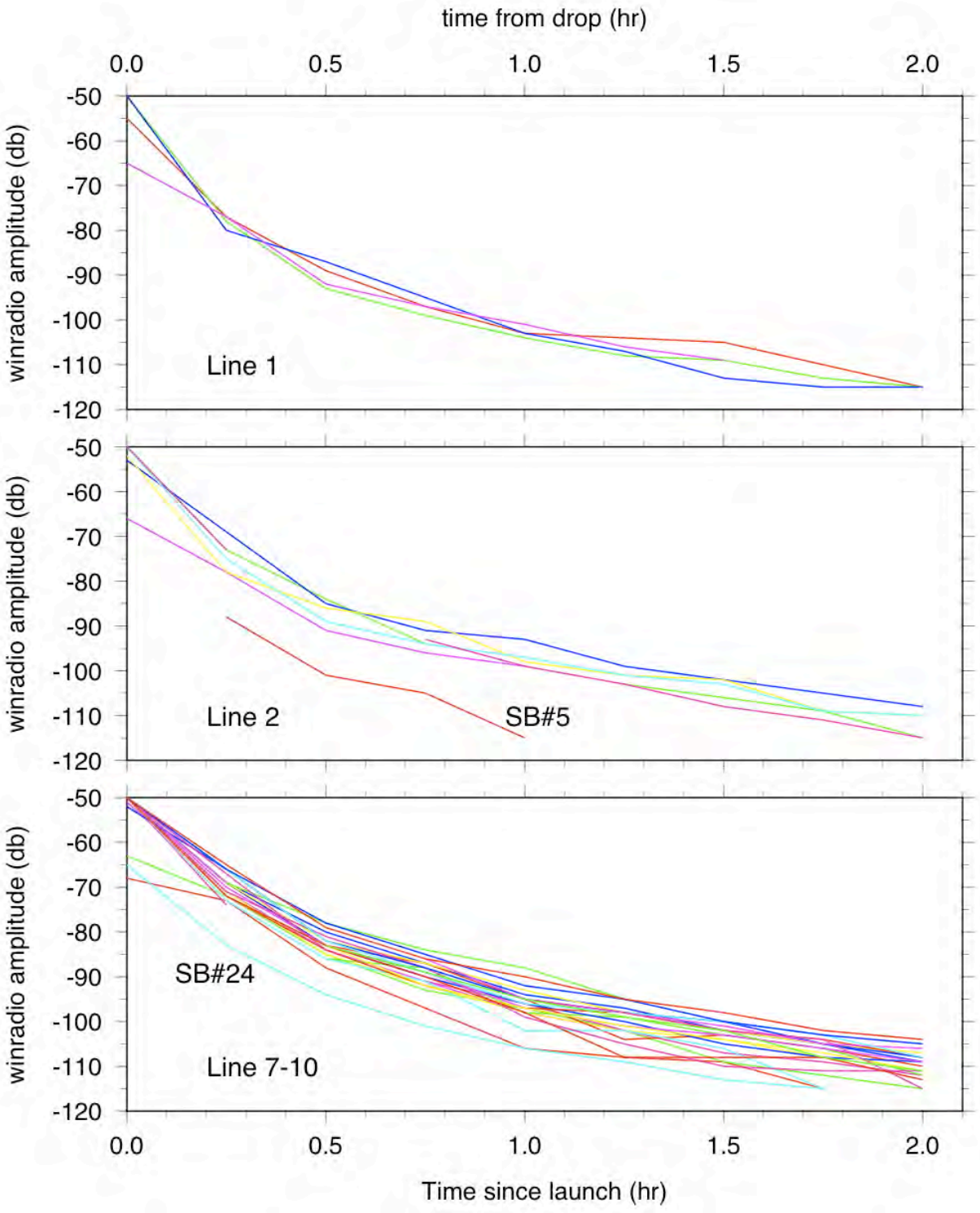

Figure 24. Plots showing the decay with time in the amplitude of the Win Radio signal on the transmission channel

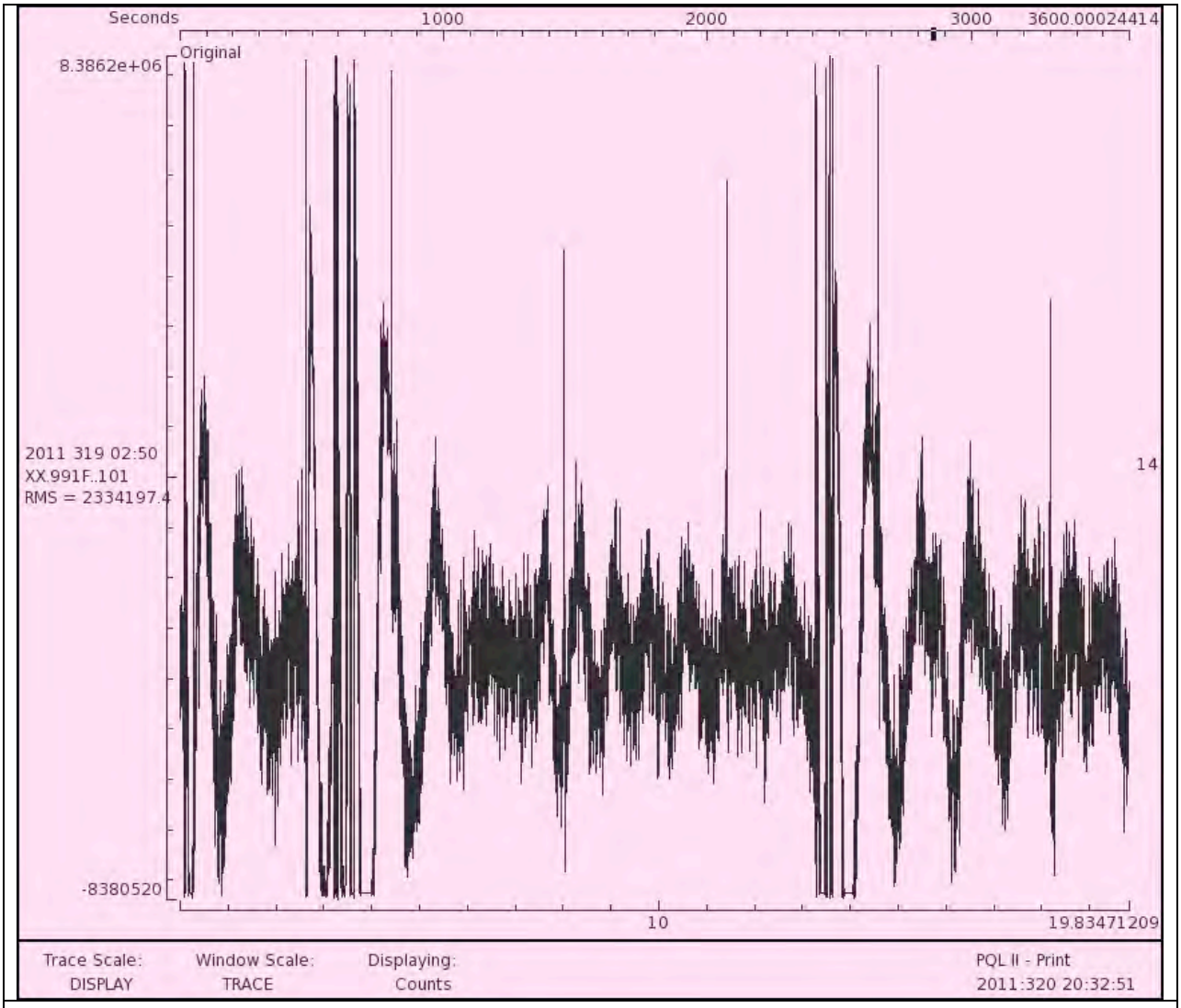

Figure 25. A sample time series of the noise on a sonobuoy record recorded after the airguns had been turned off at the end of Line 1.

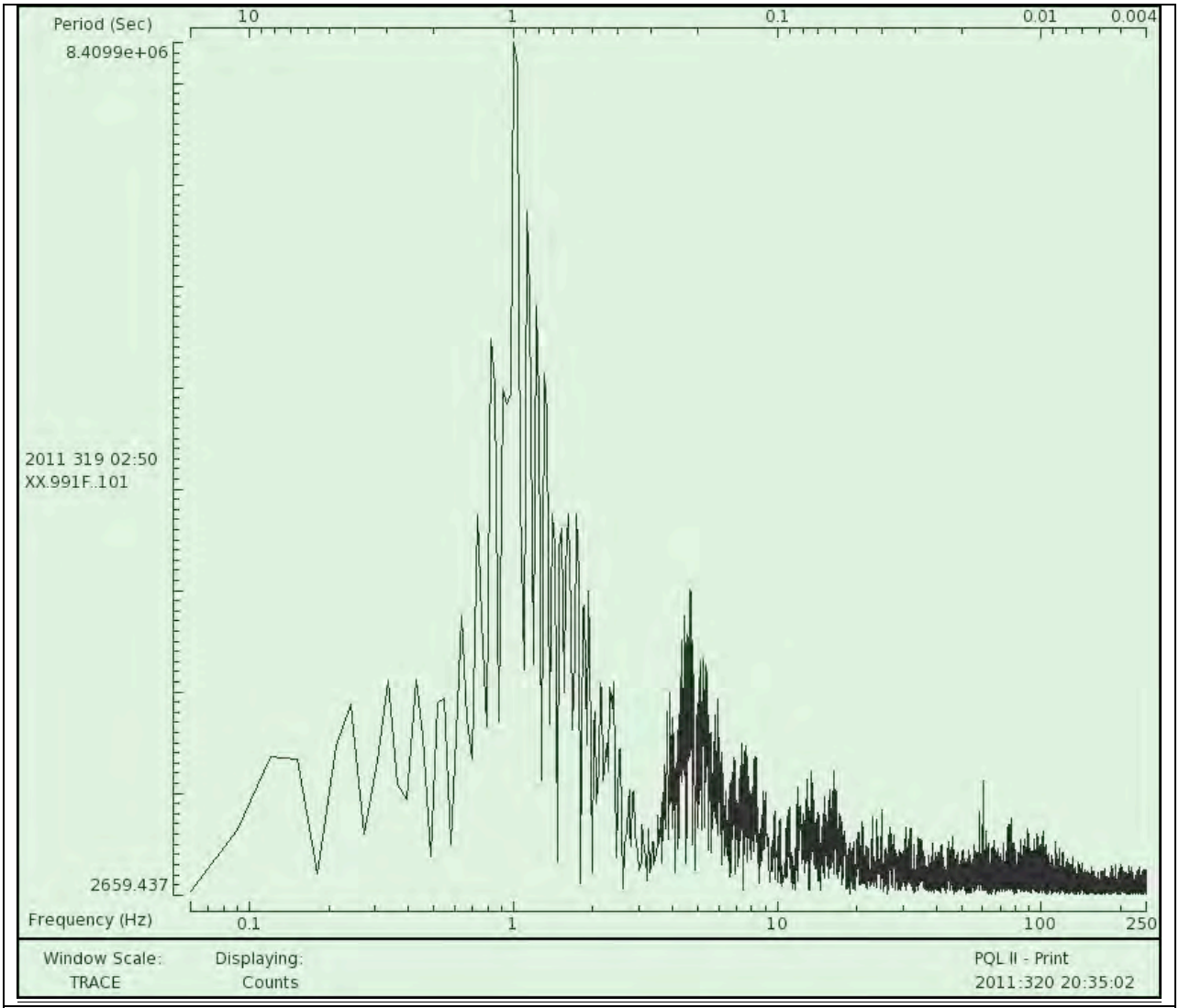

Figure 26. A sample spectrum of the noise on a sonobuoy record recorded after the airguns had been turned off at the end of Line 1.

Line 2

Thirteen sonobuoys were launched, but only 8 buoys provided adequate signal. No seismic signal was seen on SB 11. We initially observed good data on the MCS monitor for SBs 7, 8, 10 and 17, but the signal terminated after ~5 minutes. On all five bad buoys, the amplitude seen in the WinRadio display jumped at the start and decayed normally with time indicating that the buoy transmitter sending the carrier frequency functioned normally. It is possible that the connection between the hydrophone at depth and the transmitter at the sea surface was cut or damaged by a wing of one of four birds mounted on the streamer. But no wires were found when the birds were recovered at the end of the line. Despite the lack of debris, our experience at the beginning of Line 7 indicates that the cause of premature termination of sonobuoy data was indeed cutting of the hydrophone wire by a

streamer bird. Interestingly, the 1-2 sec long noise chirp centered at 1 Hz continued to appear even when the seismic signal did not, so the source of the chirp is unlikely to be in the marine environment. Moreover, the chirp does not stop when the Knudsen echosounder is turned off.

A large time gap occurred in MCS shooting between the end of Line 2 Part 1 (04:43:28/321) and Part 2 (05:01:06/321) when the ship drifted off the shooting line pre-set in the MCS navigation software (HyPack). This gap happened during SB#7, for which there were no seismograms recorded (Table 7).

At the beginning of Line 2, Hydrophone depths D2 and D3 were used on SBs 5-11 to try to reduce noise seen SBs 2-4, which were deployed using D1. We were not able to detect a change in noise level, although we had no way to quantitatively compare noise levels while recording data. In despair, we switched back to D1 after the fourth bad sonobuoy and obtained good data for five sequential buoys.

Lines 7-10

The remaining 33 sonobuoys were deployed during four days of shooting (Table 7). The MCS data was broken into four segments (Lines 7-10) to allow easier processing. Recording was stopped for a few shots during these line number changes, so sonobuoy data recorded on the MCS auxiliary channel was lost (Table 8). Gaps at these breaks in line number are too short to appear in the plots of channel gathers (Appendix 5). Fortunately, recording on the RT130 was continuous. A presumed electrical short caused the airguns to shut down for ~5 minutes beginning at 00:00:30 on JD 334. The shutdown is the reason for the break between MCS Lines 10 and10A. Since the airguns were shutdown there is a gap in sonobuoy data recorded by both the MCS and the RT130 systems. The break occurs at the end of SB 47.

Sonobuoy 18 followed the now familiar pattern from Line 2 of sending data for 4-5 minutes and then stopping. Changing hydrophone depths at the beginning of Line had produced no relief. So we moved the deployment site from the starboard 02 deck to the port 02 deck. We had no further failures, except for SB 32, which was a complete dud - no carrier frequency was seen. This success was not anticipated because both the wind and the ADCP surface current flowed from the NE to SW and, thus, moved from port to starboard. We initially thought the surface current would carry sonobuoys deployed off the port side of the ship into the airguns and streamer. Observations of the flow of water around the stern offered an explanation presented in Figure 28. Because the wind and current were constantly trying to shift the boat to the west off the shooting line, the DP system turned the orientation of the ship's bow to port. Thus, the ship's stern was turned to starboard towards from its direction of motion. The most obvious evidence of this was the deflection of the airgun and streamer tail buoys to port. The more significant effect was an asymmetric flow of water around the stern of the ship and into the wake. There was clearly more flow from the starboard side than from the port as schematically shown in Figure 28. We suggest that this flow would more often carry sonobuoys launched from the starboard side into closer proximity to the streamer than those launched from the port side. The buoys launched from the starboard side that were successful were those that

were thrown farther from the ship and those that were fortunate to be thrown just when the yaw of the ship placed the launcher farthest to starboard.

Results

Sonobuoy seismograms recorded on the auxiliary channel of the MCS system were stripped from the segd files and saved in segy format by line number (Table 8). Appendix 5 contains plots of shot gathers for all sonobuoys. In order to provide an indication of sediment thickness that could be used in preliminary interpretation of the MCS reflection profiles, we picked travel times to the seafloor at vertical incidence and at the point along the wide-angle seafloor reflection where crustal energy breaks out from the seafloor. As an example, the arrows in Figure 18 show where these points occur for SB 3. This difference in time was useful in identifying laterally coherent seismic reflected energy as basement on Line 2.

The difference in travel time between the seafloor reflection at vertical incidence and at the point where refracted energy breaks out is an indication of sediment thickness. Occasionally, more than one crustal breakout could be discerned, although the early breakouts are often faint, poorly defined, confused by hyperbolic diffractions, or offset by only a small time increment from the later crustal breakout. As an example, arrows in Figure 29 show three travel times picked for SB#12 in which both a shallow and deeper crustal refraction could be identified. Picked travel times are listed in Table 8 and plotted in Figure 30 as a function of sonobuoy number and latitude at launch. Due to the uncertainties, these interpretations are preliminary and were only used to guide shipboard interpretations of the MCS records prior to formal modeling and interpretation of sonobuoy record sections in a shore lab. At the base of the figure, an arbitrary index of the amplitude of the main crustal refractor is also plotted. This scale varies from zero for buoy records in which no refracted energy could be observed to five for the strongest appearing refraction. Two refracted arrivals could be identified in six sonobuoys. Sonobouy 12 (Figure 29) on Line 2 presents the most reliable evidence of an igneous sill layer within the sediment layer.

We also examined details of specific portions of the seismograms by plotting time series for individual shots. Spectra were computed on these segments to identify the frequencies present in various arrivals. Figure 31 shows traces and spectra for the water wave arrival recorded with a hydrophone depth of 30 m. We selected the records from three sonobuoys that had particularly long-lived direct waves and relatively low noise. These water-wave arrivals represent energy traveling nearly horizontally for 2-3 km. Unlike energy traveling vertically down to the seafloor, these arrivals may include multiple interactions with the sea surface. For all three sonobuoys, the direct arrivals include 2-3 wavelengths with relatively similar amplitudes and periods of 10-12 ms. As a result, the spectra peak at 110 Hz. The spectra are remarkably flat from 5 Hz to above 130-140 Hz. The high frequency rolloff occurs below that of the Krohn-Hite anti-alias filters (150 Hz) and is, thus, a feature of the airguns and the interaction with the sea surface rather than the filters.

To determine if the depth of the hydrophone influences the seismograms, we plotted traces and spectra in Figure 32 from three sonobuoys spaced closely along Line 2 for which three different hydrophone depths (30, 61, and 122 m) were programmed. As in Figure 31, the

arrivals include 2-3 wavelengths with periods of 10-12 ms. Unlike the seismograms in Figure 31, the maximum amplitude of the 2-3 pulses increase with time shifting energy to longer wavelengths. As a result, the spectra peak below 100 Hz. Hydrophone depth appears to have little effect on either the traces or the spectra. The spectra for seismograms recorded with the hydrophone at 30 m (sonobuoy 12) are unusual in having a shallow notch at 80-90 Hz. This notch does not appear in any of the spectra in Figure 31 that were also obtained with the hydrophone set to 30 m. Thus, the primary source of variability is unlikely to be hydrophone depth and more likely some feature of the sea surface (swell amplitude, direction) or small variations in the operation of the airguns.

To examine the sediment reflections, Figure 33 shows seismograms for three sonobuoys recorded for ~0.6 s after the seafloor reflection. All seismograms were obtained at short range (~0.4 km) with the hydrophone set to 30 m depth. The traces are remarkably similar over the initial 30 ms indicating that the down-going pulse was similar. Despite the widely varying traces after the initial 30 ms, the spectra are also remarkably similar. Thus, the notches at 30, 60, and 90 Hz are likely features of the downward traveling source signature. The high frequency roll-off occurs at about 105 Hz, which is only about 20 Hz less than the roll-off frequency of the direct wave spectra in Figures 32 and 32.

To determine if the seismograms recorded by sonobuoy hydrophone differed significantly from the processed MCS seismograms, we show in Figures 34 and 35 the near-vertical incidence seismograms from two sonobuoys with CDP stacked with the same shots from two versions of processed MCS The most remarkable feature of these plots is the similarity between sonobuoy and the MCS traces. Clearly MCS processing improves the resolution of sedimentary reflections. But the phases of individual waveforms are very similar. Spectra of the two data sets were also similar particularly those for SB#50 (bottom frame) in which the spectral notches line up. The spectra, however, initially differed at the low frequency end. In Figure 34, the MCS data (labeled "new" in the data archives) were processed with a bandpass of 20/30-180/200 Hz, whereas in Figure 35, the MCS data (labeled "final" in the data archives) were processed with a bandpass of 5/8-180/200 Hz. Spectra computed on the former data set roll off 15-20 Hz above the low frequency end of the sonobuoy spectra (Figure 34). Test MCS plots indicated some deep reflections were better imaged when the bandpass of MCS processing was expanded downward to 8 Hz (Figure 35).

A significant goal of the sonobuoy component of the survey was to identify the depth to basement and any igneous sills within the sediment sections. Shore-based processing will include efforts to better image arrivals that reveal the nature of basement features. To assist this effort, we more closely examined the refracted arrivals in three sonobuoys from which these arrivals were relatively strong. Time series and spectra for 0.45 sec intervals in Figure 36 show that the crustal refracted arrival comprises frequencies in the 10-15 Hz band. Time did not allow further examination of the features of the sonobuoy data in this passband.

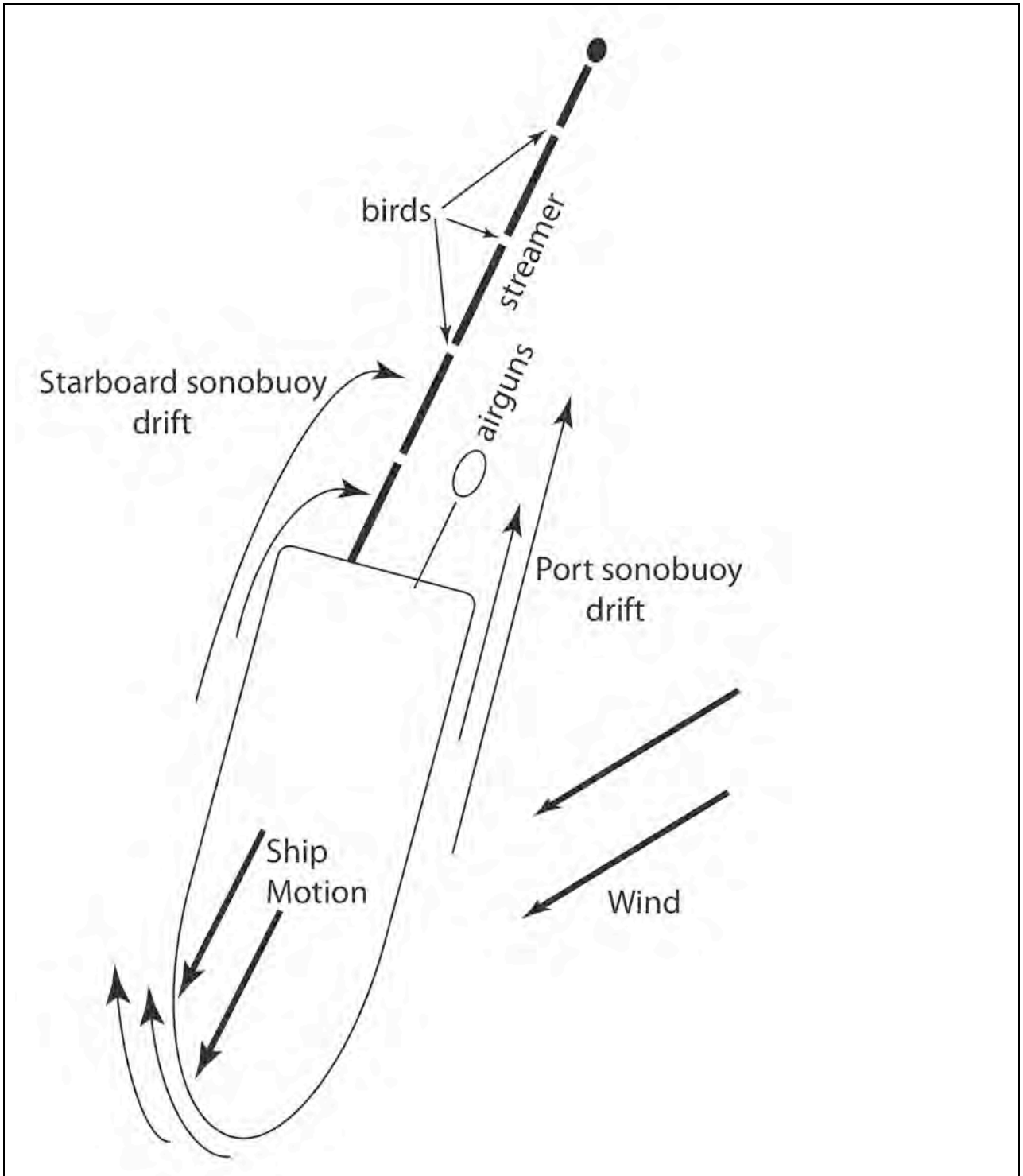

Figure 27. Cartoon showing the ship orientation relative to the sonobuoy during noise tests after the airguns had been turned off at the end of Line 1.

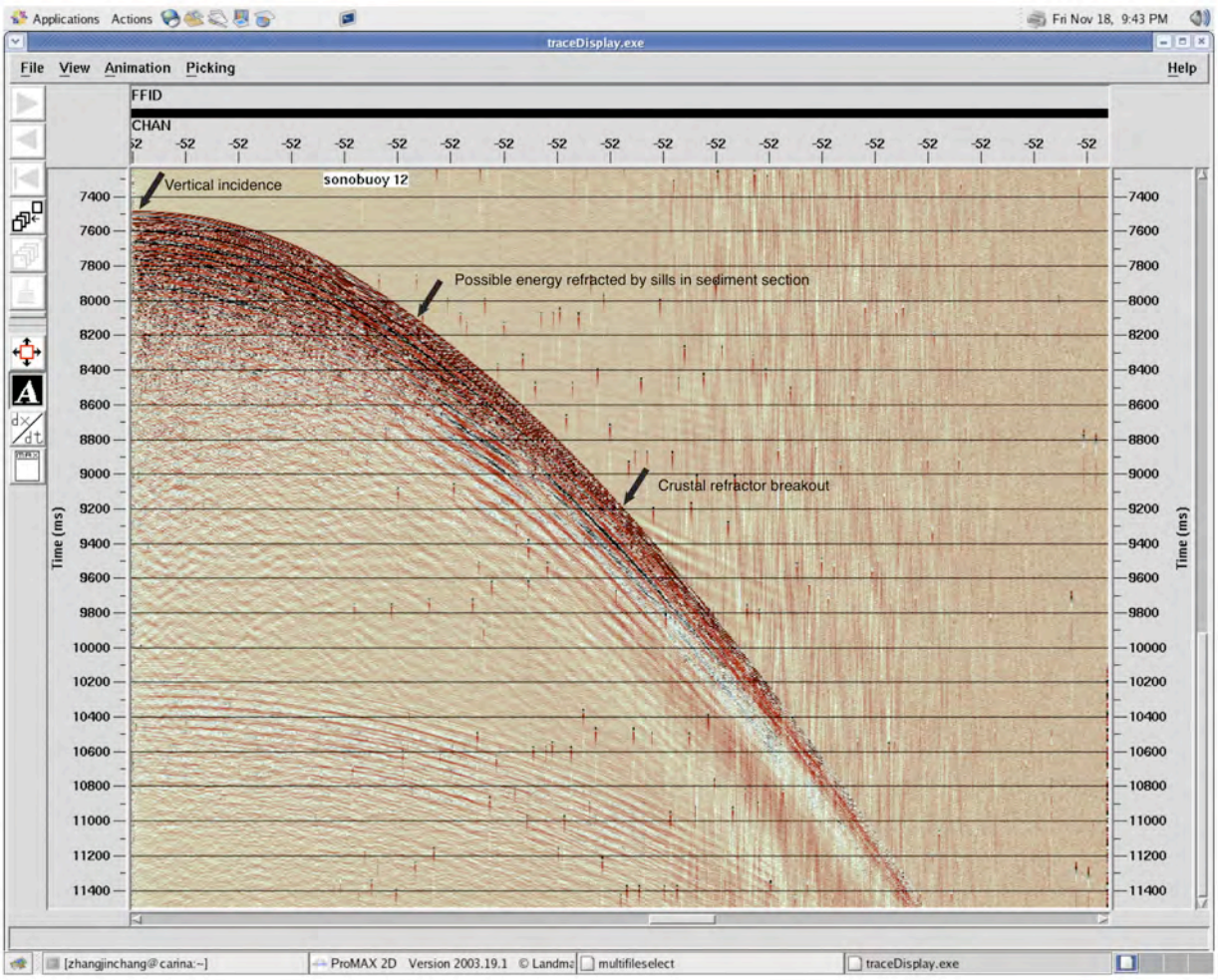

Figure 28. Exampleof sonobuoy record SB12

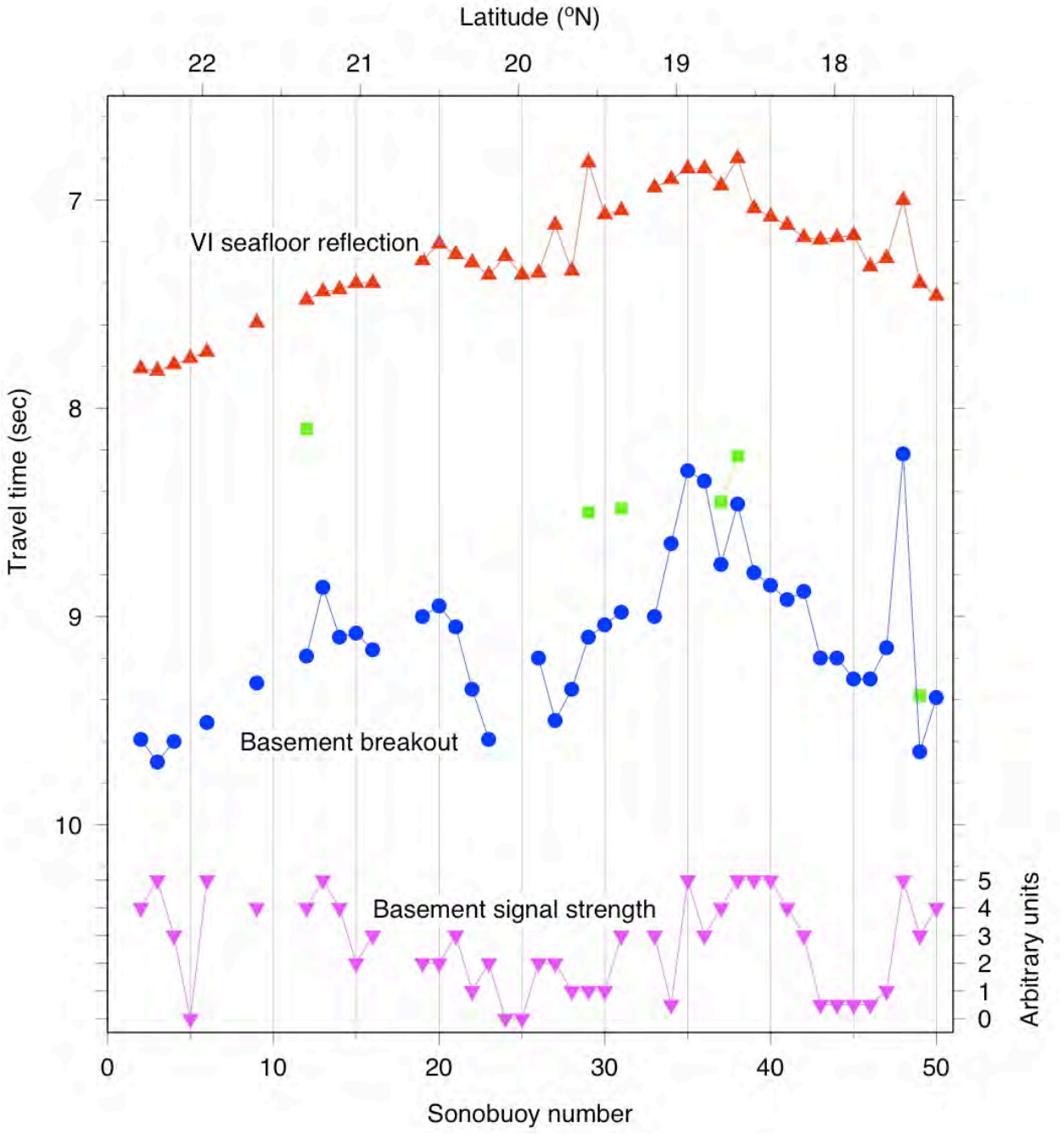

Figure 29 Picked travel times plotted as function of sonobuoy number and latitude at launch.

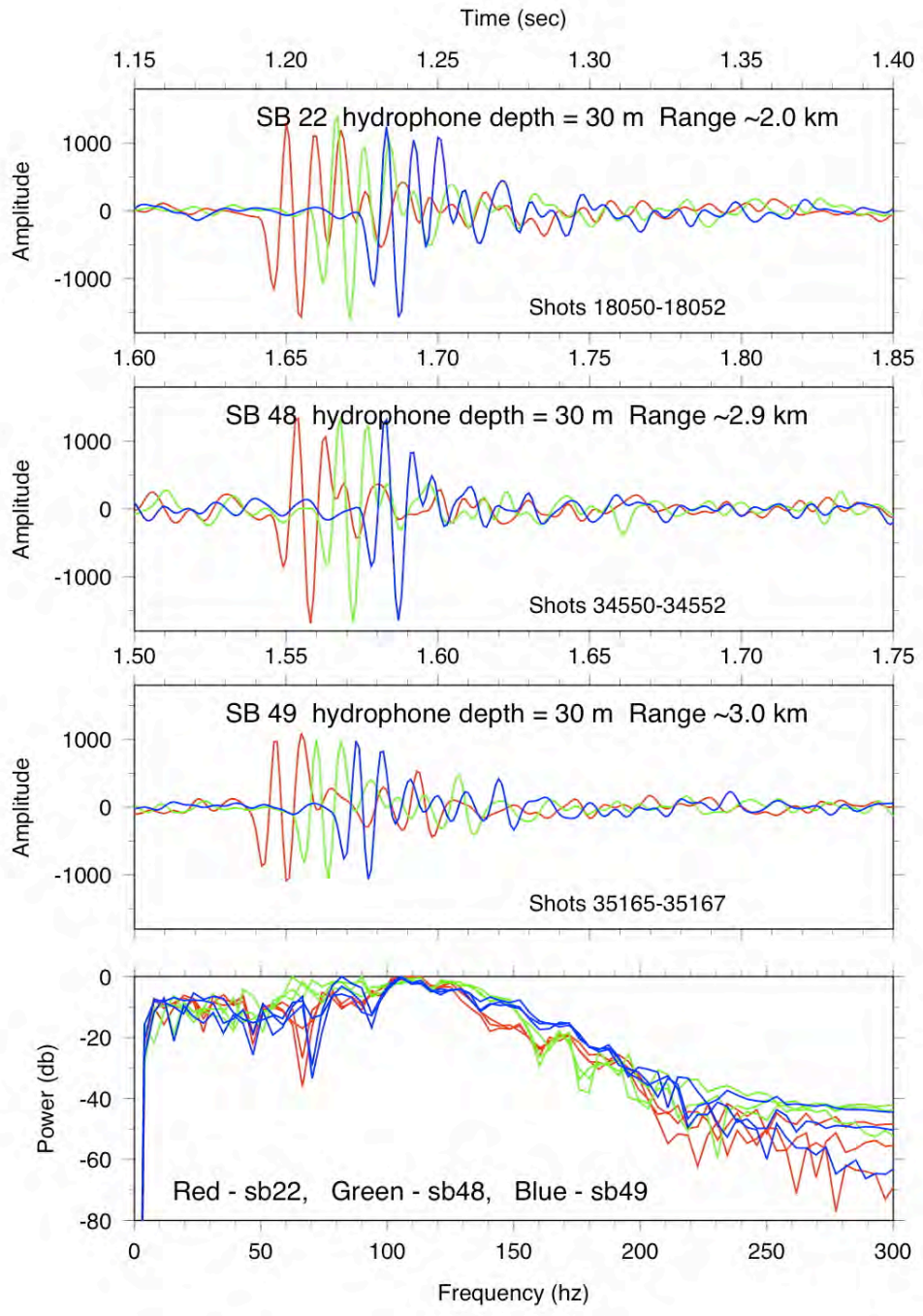

Figure 30. Traces and spectra for the water wave arrival on sonobuoy records.

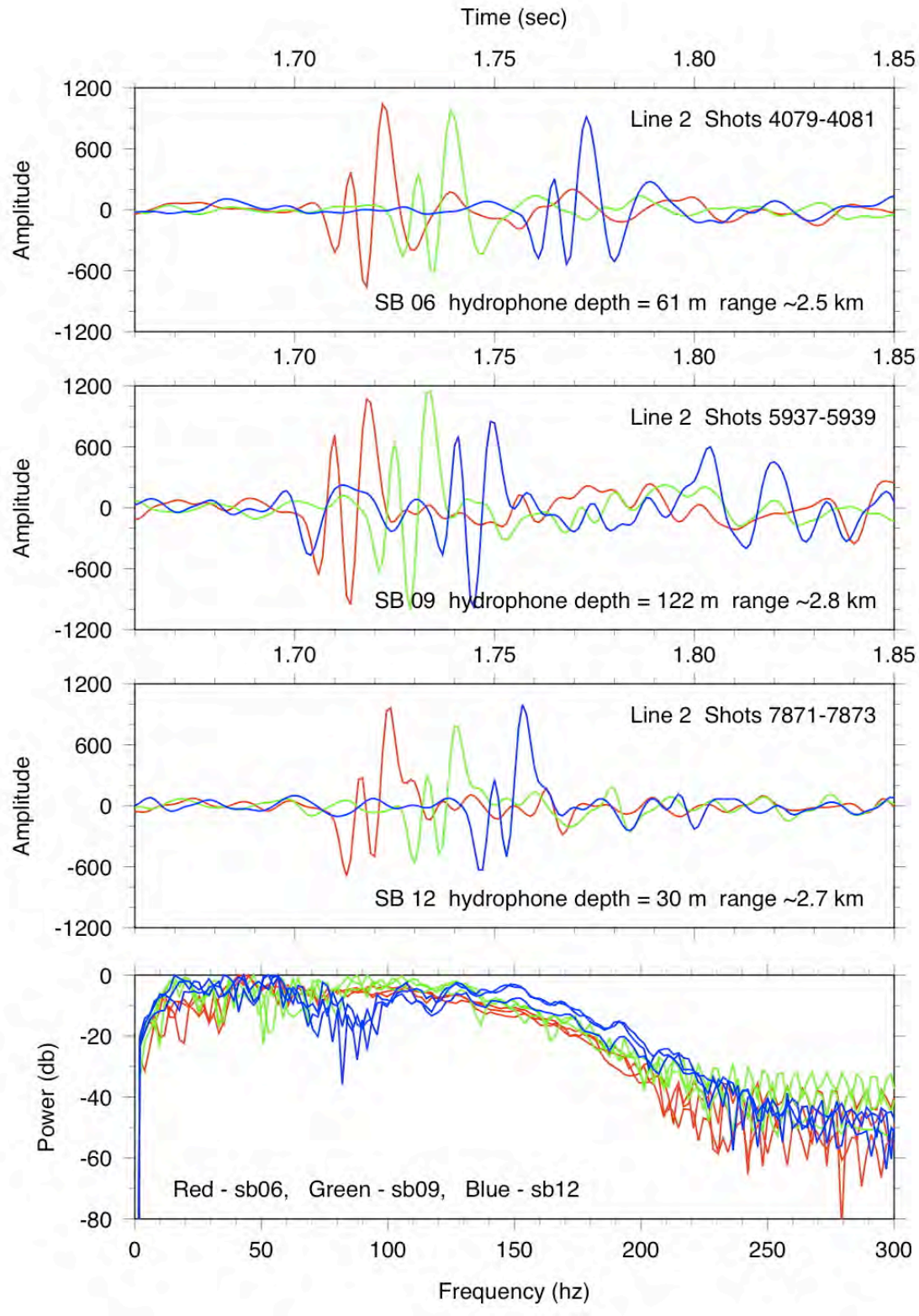

Figure 31. Traces and spectra for three sonobuoys at different depths

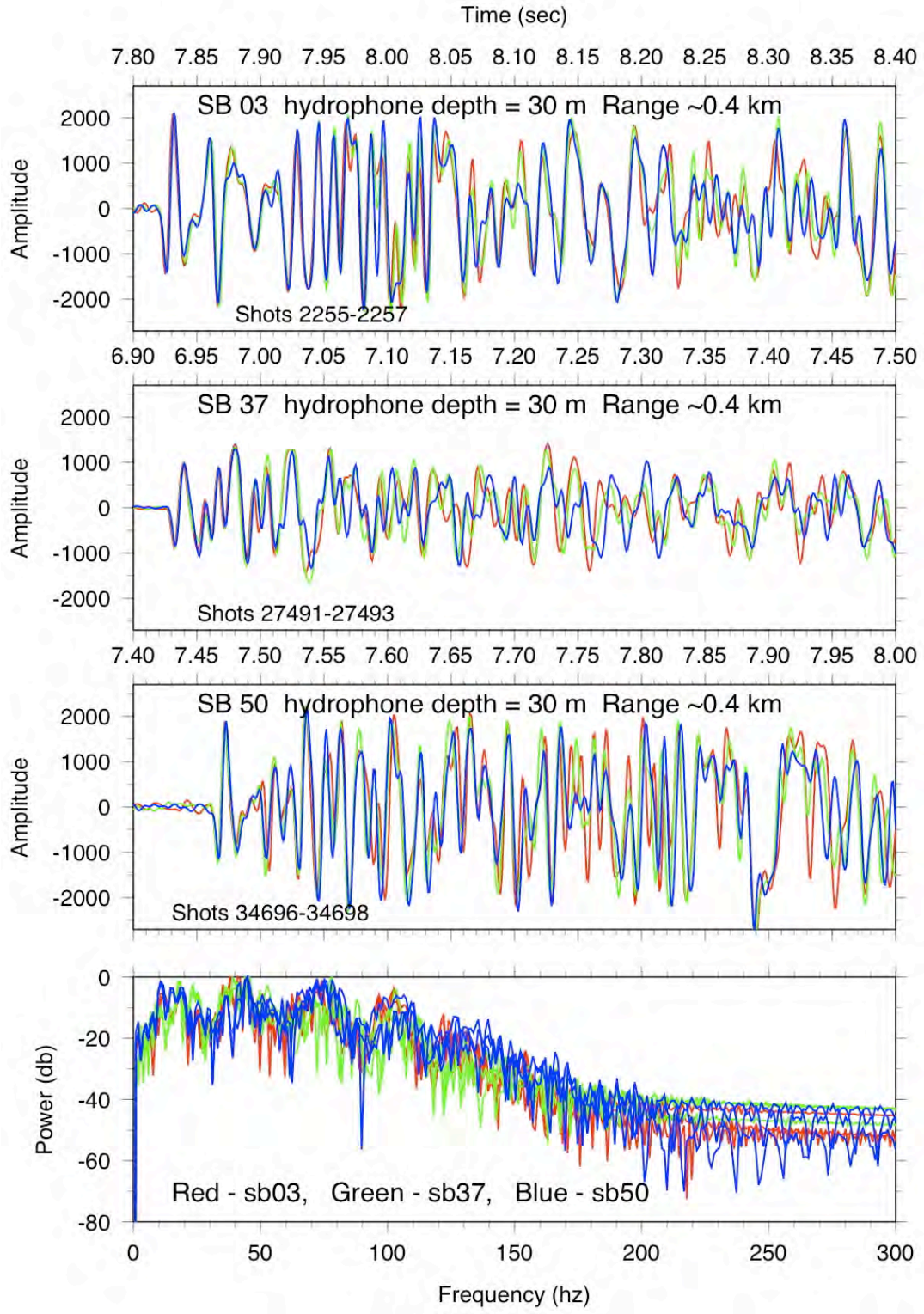

Figure 32. Seismograms for three sonobuoys over 0.6 secs

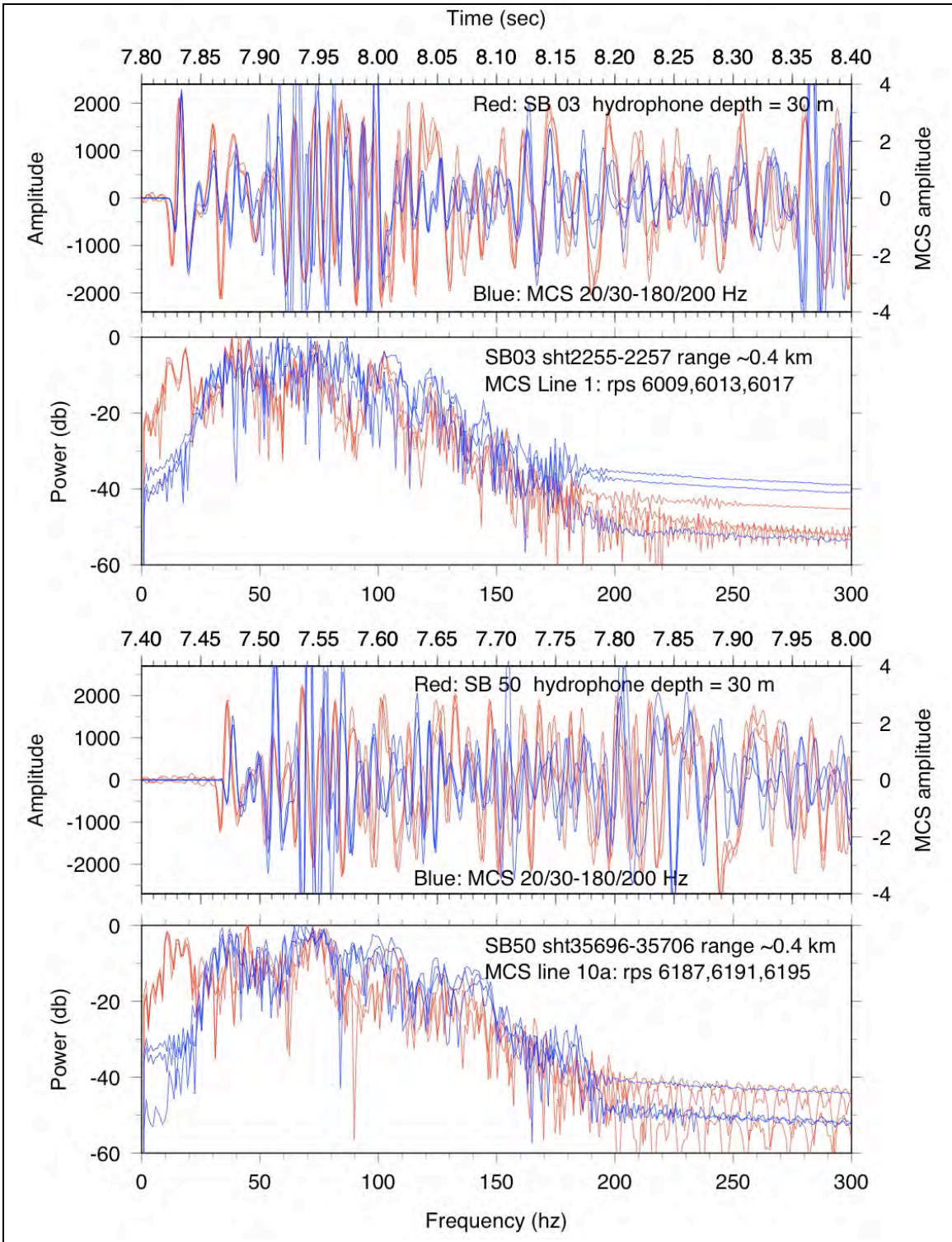

Figure 33. Near vertical incidence seismogram for MCS data compared to SB03 and SB50

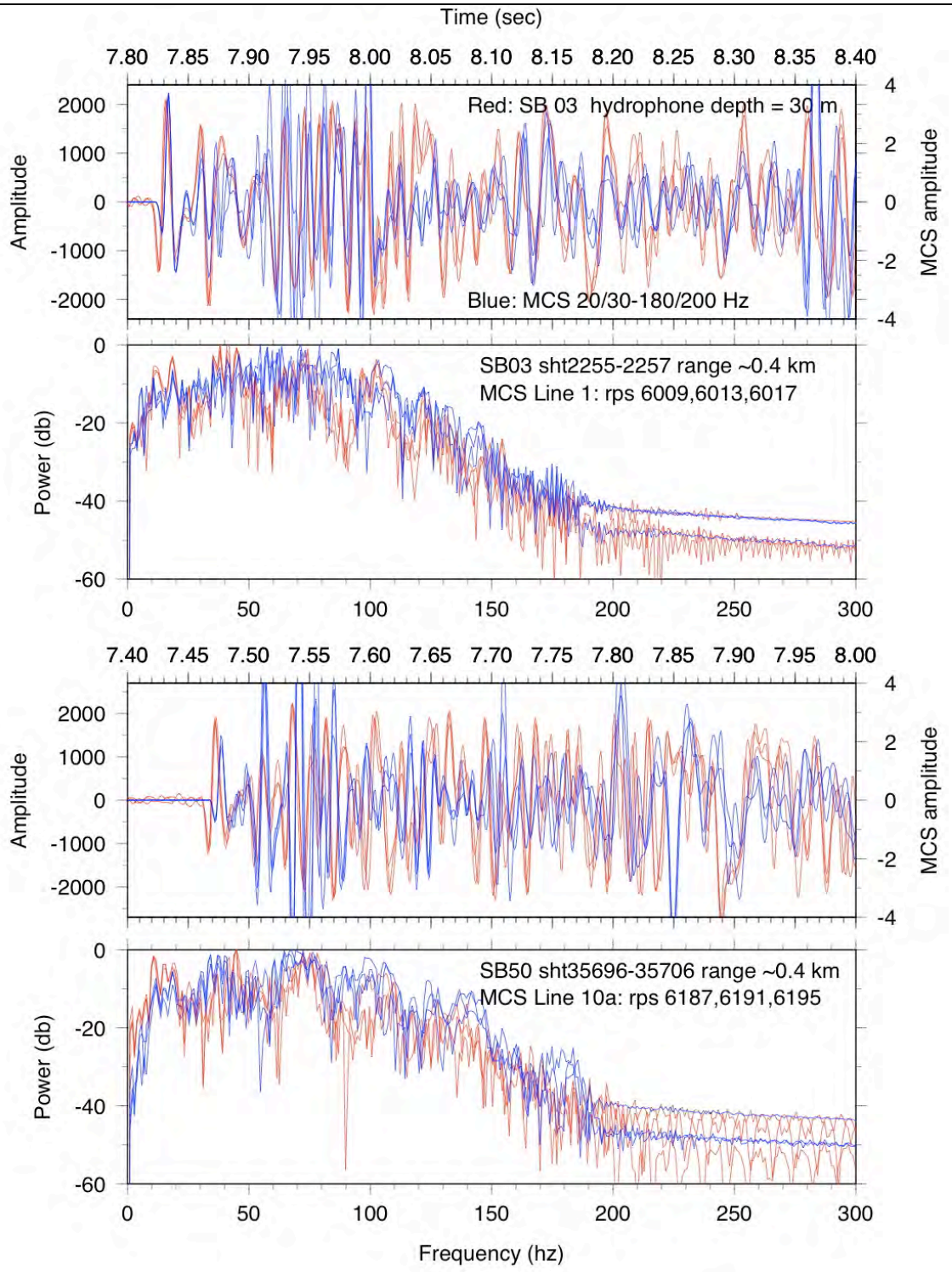

Figure 34. Near vertical incidence seismogram for MCS data compared to SB03 and SB50

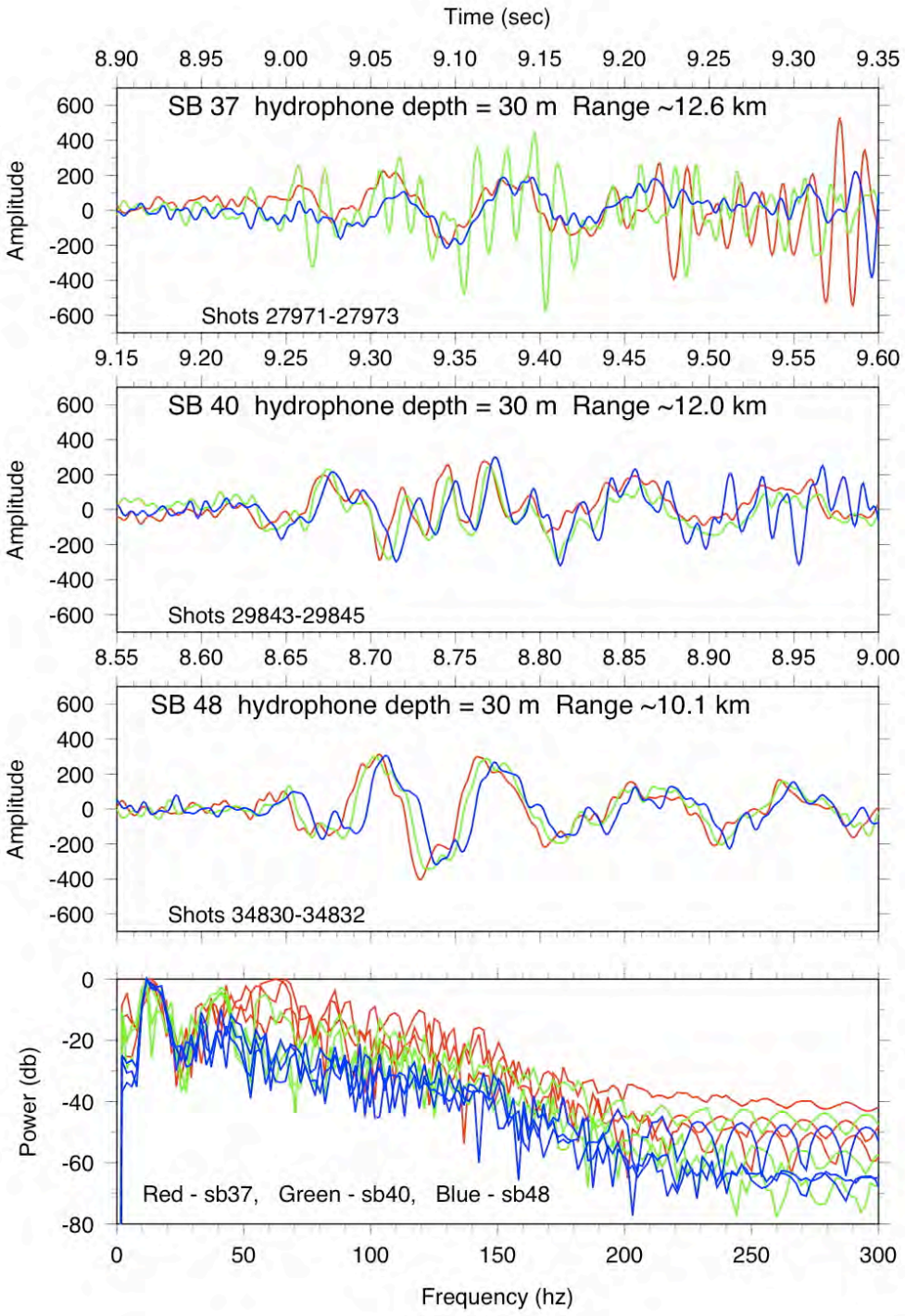

Figure 35. Time series and spectra for SB37, SB40, SB48 at 0.45 sec intervals.

8. Broader Impacts

Exposure to Field Oceanography

One of the major goals of this NSF project was to expose young scientists to field oceanography, providing them the opportunity to participate in cutting edge research with scientists in all stages of their careers. This sea-going experience has provided hands-on training in geophysical data acquisition, processing and interpretation.

Five undergraduate students from Kutztown University (KU) participated in the Jurassic Quiet Zone cruise as geophysical watchstanders. KU is a public, undergraduate liberal arts college in eastern Pennsylvania where 42% of students are first-generation college students. These students were joined by three recent graduates from Boston College, Juniata College, and the University of Maine, Orono. Each received bachelor's degrees in earth science in 2011, and one had begun her PhD program at Purdue.

By the time we reached Guam, the eight young scientists had stood watch in shifts (four on eight off) 24-hours a day for 40 days. During their shifts, they regularly monitored the gravimeter, surface towed magnetometer, Knudsen CHIRP SONAR system, and EM-302 multibeam bathymetry system. They logged ship speed and course over ground, depth to seafloor and position every 15 minutes. They also processed and gridded the multibeam data using MBSystems and Generic Mapping Tool (GMT). Dr. Adrienne Oakley served as the geophysical team lead on this cruise. The watchstanders, under the direction of Dr. Oakley, were responsible for creating daily reports which summarized the geophysical data collected including: CHIRP, bathymetry, backscatter, ship's track, and multichannel seismic. These reports were used by the chief scientists and Sentry team to plan AUV dives, refine survey waypoints, and make initial interpretations.

In addition to their duties in the computer lab, the watchstanders helped to deploy and retrieve gear (including sonobuoys, XBTs, surface-towed magnetometer, TowCam and seismic), assisted in data reduction and processing, and attended science briefings given by the chief scientists. All of the students spent many hours on deck deploying and retrieving seismic gear and the surface magnetometer and helping to repair the seismic streamer. During seismic operations the watchstanders assisted the Scripps team and Dr. Oakley in monitoring data acquisition and keeping constant radio contact with the protected species observers on deck. During AUV-Sentry and TowCam dives, they logged and plotted the position of the ship, the position and depth of the AUV, the depth of the TowCam sled and the tension on the cable. The students learned to plot the ship's hourly position in ArcGIS as well as by hand on large charts. Early in the cruise, plotting hourly position by hand allowed the watchstanders to catch and correct an important navigation error.

On top of their cruise duties (watchstanding and the daily blog), the KU students needed to find time to do homework, labs and even exams while on board the R/V Thomas G. Thompson. The undergraduates received three college credits (either as research or an internship) for their time on the research cruise. Their other nine credits for the semester were taken on campus. Faculty at Kutztown worked with Oakley to arrange schedules, and rearrange courses, for the students to ensure that their academics would not suffer even

though they missed the last five weeks of the fall semester. The students all took on extra work earlier in the semester and some whose classwork could not be completed while at sea, received an incomplete in courses which they will finish over winter break.

In living and working on a research vessel, the young scientists also learned from the crew aboard the R/V Thompson. The watchstanders stood bridge watches under the supervision of the captain and mates to see the interplay of scientific operations with ship operations and navigation. In the pilot house they "drove" the ship, plotted the course and calculated distances, learned about the ship's RADAR systems, and spent quality time with those in charge of the Thompson. Captain Patrick Donovan gave a lecture and demonstration on celestial navigation by sextant. Some of their blog topics involved ocean engineering, water production and waste management on board. These blogs required the students to interview the crew and tour the engine rooms, incinerator and other usually restricted areas of the ship. Because of these opportunities, the students learned what goes into making our water run, lights work, toilets flush, and all of the other day to day activities that we took for granted on board.

The cruise provides an incredible networking experience for our students. Because this cruise involved many different components (AUV-Sentry, multi-channel seismics, towed magnetometers, protected species observation) the students worked with scientists and technical experts from across the US. They were directly involved in cutting-edge science that pushed the limits of current technology, working in some of the most remote regions of the planet. They witnessed the work that goes into designing a successful oceanographic survey, and gained an understanding of the challenges of doing research at sea (e.g. bad weather, system malfunctions, troubleshooting deep-sea communications and navigation). In short, this research experience has significantly enhanced their undergraduate education.

Enhancing Scientific and Technological Understanding through Outreach

A further goal of this research is to provide resources for community outreach. In our NSF project description we proposed to try to broadcast live from the ship back to the Kutztown campus in order to connect to a broader audience. Limited internet bandwidth and ship headings that were incompatible with our satellite connections, made this impossible. However, prior to the cruise, Tominaga and Oakley decided that a cruise website and blog would better serve our outreach goals and reach a much larger audience than an occasional broadcast. KU and WHOI combined resources to support the travel expenses of Dr. William Koeppen, who created the website and managed the blog while at sea. Since this was not a component of the original proposal, there was no money to support Dr. Koeppen's work on the cruise and prior to it, and he donated his time and efforts.

As part of our dedication to maximizing the broader impact of the TN272 research cruise, we created, advertised, and maintained a public website: http://www.kutztown.edu/JOCMS2011. The site contains static pages describing the background, methods, and purpose of the expedition as well as a personnel list for the science party with names, affiliations and headshots. It also contains a dynamic blog page that was updated six days per week with reports written by Kutztown University students,

corralled and edited by our media coordinator. The reports were targeted to an audience of educated adults, and they detail the students' understanding of the ship's operation, instrument design and construction, vehicle deployments and retrievals, and daily life aboard the Thompson.

All of the website's pages were coded from scratch using HTML and CSS by the media coordinator. We explored other possibilities (e.g., Wordpress, Joomla, etc.) but found that they did not meet our design standards, would require too much bandwidth to be stable over HiSeasNet, or would need continuous technical support from the shore. Images and diagrams on the static portion of the site were obtained with permission, taken from the public domain (e.g., Wikipedia), or created outright. Photographs accompanying the dynamic blog pages were taken and edited by the media coordinator while on board. At the end of the cruise on December 17th, 2011, the site contained ~50 pages of background text and student reports along with ~150 images from the trip.

Our cruise website (www.kutztown.edu/JOCMS2011), with over 1000 unique hits in the first week, has been viewed across the nation and in several countries worldwide. In particular, the student blog was extremely successful (www.kutztown.edu/jocms2011/blog.html). The KU students each wrote blog per week on a variety of topics including the goals of the research, scientific theory, the technology used on board (e.g. AUV-Sentry, seismic refraction, Thompson engineering), as well as their personal experiences at sea (e.g. a day in the life of a watchstander and seasickness). The students learned scientific reporting under the tutelage of Drs. Adrienne Oakley and William Koeppen. This type of writing is extremely challenging and most had not been exposed to it before this cruise. The student writing improved as the cruise progressed and their ability to understand technical subjects and make them accessible to the general public became apparent. By the mid-way point of the cruise (Day 21) we had over 2000 visitors and 11,000 page views. Trend analysis shows that the average time spent on the site by each visitor was 4.5 minutes, indicating that the blogs were read in their entirety. Creating and managing high-impact outreach material is a full-time job on a research cruise.